Proceedings: Fourth International Conference on Case Histories in Geotechnical Engineering, St. Louis, Missouri, March 9–12, 1998.

SOIL DILATION AND SHEAR DEFORMATIONS DURING LIQUEFACTION

Ahmed-W. Elgamal
Univ. of California, San Diego
La Jolla, CA-USA 92093

Ricardo Dobry
Rensselaer Polytech. Instit.
Troy, NY-USA 12180

Ender Parra
INTEVEP, SA
Venezuela

Zhaohui Yang
Columbia University
NY, NY-USA 10027

ABSTRACT

Paper No. 3.24

Recent records of seismic site response have documented a salient liquefaction-induced cyclic shear-deformation mechanism. During liquefaction, these ground acceleration records have suggested a possible strong influence of soil-skeleton dilation at large cyclic shear strain excursions. Such phases of dilation can result in significant regain in shear stiffness and strength, leading to: i) associated instances of pore-pressure reduction, ii) appearance of spikes in lateral acceleration records (as a direct consequence of the increased shear resistance), and iii) a strong restraining effect on the magnitude of cyclic and accumulated permanent shear strains. As presented in this study, these response effects are also thoroughly documented by a large body of experimental research (mainly employing clean sands and clean non-plastic silts), including centrifuge experiments, shake-table tests, and cyclic laboratory sample tests. A number of efforts to computationally simulate this aspect of soil behavior are presented. In addition, the framework for a newly developed computational model is discussed.

KEYWORDS

Liquefaction, cyclic-mobility, sand, dynamics, constitutive modeling, earthquake, dilation, soil, plasticity

INTRODUCTION

Recent records of seismic site response have documented a salient liquefaction-induced shear-deformation mechanism. In particular, these ground acceleration records suggest a possible strong influence of soil dilation at large cyclic shear strain excursions. Such phases of dilation can result in significant regain in shear stiffness and strength, leading to: i) associated instances of pore-pressure reduction, ii) appearance of spikes in lateral acceleration records (as a direct consequence of the increased shear resistance), and most importantly, iii) a strong restraining effect on the magnitude of cyclic and accumulated permanent shear strains. This restraint on shear strain has been noted and referred to as a form of cyclic-mobility in a large number of pioneering liquefaction studies (e.g., Seed and Lee 1966, Casagrande 1975, Castro 1975, Castro and Poulos 1977, Seed 1979). For the important situations of biased strain accumulation due to an initial locked-in shear stress, this pattern of behavior may play a dominant role in dictating the extent of such deformations.

In addition to the evidence provided by recorded seismic response (which is still scarce), the above mentioned effects are also thoroughly documented by a large body of experimental research (employing clean sands and clean non-plastic silts), including centrifuge experiments, shake-table tests, and cyclic laboratory sample tests. In this paper, a summary is provided of the relevant: i) seismic response case histories, ii) recorded experimental response, and iii) constitutive models developed to address this phenomenon. In addition, the framework of a newly developed computational model is presented and discussed.

DILATION

In general, at low confinement levels, dense granular soils exhibit a dilative response when subjected to shear loading conditions (Lambe and Whitman 1969). Under cyclic shear excitation, a sand mass will undergo this coupled shear-dilation process in a manner analogous to that shown in Fig. 1 (Youd 1977). In a saturated state, the dilation-induced increase in volume is accommodated mainly due to the migration of fluid into the created additional pore-space. The relatively low soil permeability (and/or the relatively fast rate of loading) will hinder this water migration process resulting in: i) an immediate reduction in pore-water pressures and associated increase in effective confinement, and ii) a resulting possible sharp slow-down of the deformation process. This slow-down occurs due to: i) the slow-down in dilation (and consequently in the coupled shear straining process), which is directly proportional to the rate of inward fluid flow, and ii) the instantaneous increase in soil stiffness resulting from the increase in effective confinement (due to pore-pressure

reduction). In the following sections, a set of recorded responses is shown, in which dilative effects appear to have played a major role.

UNDRAINED CYCLIC LABORATORY TESTS

The mechanism of interest may be illustrated by the response shown in Figures 2 and 3 (Arulmoli *et al.* 1992, Taboada and Dobry 1992). This response is representative of a large number of undrained laboratory experiments conducted to study the cyclic behavior of Nevada Sand (with relative densities in the range of about 40%-60%).

The simple shear test (Fig. 2) shows: i) increase in shear stiffness and strength at large shear strain excursions, along with an associated increase in effective confinement (reduction in excess pore-pressure,) and ii) a cycle-by-cycle degradation in strength as manifested by the occurrence of increasingly larger strain excursions, for the same level of applied shear stress. It may be observed that as the shear strain increases, the sand skeleton is forced into dilation (soil behavior changes from contractive to dilative along the phase transformation envelope of shear strength).

The triaxial test (Fig. 3) shows the situation when an existing driving shear stress is present (Dobry et al. 1995). This existing stress forces the strain to occur in a biased preferred direction, on a cycle by cycle basis (Fig. 3). In these cycles, the dilation-induced increase in strength (shear stress) during liquefaction is seen to evolve such that a net finite increment of permanent (down-slope) shear strain occurs. The magnitude of such increments determines the total accumulated permanent deformation.

In summary, during liquefaction it may be noted that: i) the regain in shear strength (appearance of stress spike) follows a phase of softer soil response that results in yielding at very low shear strength, ii) this regain may virtually arrest further straining during a given cycle, and iii) in the presence of a driving shear stress, cyclic loading may result in a pattern of cycle-by-cycle accumulation of permanent strain increments, each ending with a stress spike.

Under conditions of dynamic excitation, a shear stress spike may be also manifested in the appearance of a corresponding spike in a recorded acceleration history. This was clearly manifested (Fig. 4) in the data of Yoshimi and Oh-oka (1975), who employed a dynamic shear testing technique (tests on fine sand from Bandaijima, Niigata at a relative density of about 37%).

Therefore, during liquefaction of a level ground subjected to cycles of uniform base excitation, a recorded acceleration history may display (Fig. 4a): i) a few acceleration spikes around the onset of liquefaction (r_u = 1.0), and ii) a possible disappearance of spikes thereafter. The spikes may disappear due to: i) further softening of the soil, thus allowing for larger cyclic deformations to occur without reaching a high enough strain to cause dilation (and a corresponding stress or acceleration spike), and/or ii) reduction in cyclic shear strains due to a base isolation mechanism created by subsequent liquefaction of underlying soil layers. In the level ground case, the spikes will be equally visible on both sides of the recorded acceleration response (with uniform cycles of excitation). When a driving shear stress is present (e.g., near the free face of a slope, behind a yielding retaining wall, or along a mildly inclined ground surface), the biased (down-slope) cyclic strains will generally be associated with larger dominant spikes (compared to the up-slope direction). This will lead to an asymmetric pattern of acceleration, which might persist during the low shaking tail end of an earthquake, denoting the continued accumulation of large cyclic deformations (lateral spreading). In this regard, the low shaking phase may allow for reversal of loading direction, and re-accumulation of an additional strain increment during a subsequent cycle.

The response depicted by Figure 2 has been documented in laboratory tests for numerous sands. Figure 5 (Seed and Lee 1966) shows two typical stress-strain loops for samples of loose and dense sand during liquefaction, where the influence of dilatancy is clearly manifested. Lee and Schofield (1988) showed a cycle of sand response (Fig. 6) as documented by Tatsuoka (1972) in triaxial test investigations. Ishihara (1985) presented stress controlled cyclic torsion shear test results that constitute one of the prime examples of dilative soil response during liquefaction (Fig. 7). Additional tests have been also reported by (Figs. 8-12) Tatsuoka *et al.* (1986), Yamashita *et al.* (1989), Hyodo *et al.* (1991), Kawakami *et al.* (1994), Shamoto *et al.* (1997) and Zhang *et al.* (1997) using Toyoura sand at a relative density in the range of about 50% to 100%. Response of the Masado soil (high quality relatively undisturbed samples) that liquefied at Port Island during the Hyogo-ken Nambu earthquake (Soils and Foundations 1996) is also seen (Fig. 13) to demonstrate a similar mechanism (Hatanaka *et al.* 1997). This mechanism of increase in soil stiffness at large strains, might partially account for the observation (Scott 1997) that most dock movement at Port Island resulted from the first earthquake acceleration peaks, not liquefaction.

SHAKE TABLE STUDIES

Dilative soil behavior has been frequently observed in shake table studies. Most of these studies were conducted in Japan. Using Toyoura sand with relative densities in the range of 68%-79%, a series of such tests was conducted by Koga and Matsuo (1990). A sample of the recorded accelerations and pore pressures is shown in Fig. 14.

Using a shear beam approach, Koga and Matsuo (1990) developed an extremely effective 1-dimensional simple procedure to calculate shear stress and shear strain histories, directly from the recorded accelerations (Fig. 14b). The calculated stress-strain histories are shown in Fig. 15. It is noted here that the observed acceleration spikes (Fig. 14) correspond to instants of reduction in excess pore pressure,

and are manifested as an increase in shear stress at large shear strain amplitudes (Fig. 15). The calculated stress-strain histories are quite similar in character to those observed in cyclic laboratory tests (e.g., Fig. 2).

Acceleration spikes similar to those observed by Koga and Matsuo (1990) are often observed in shake table tests (Fig. 16) such as those conducted by Okumura Co. (Ishihara *et al.* 1991). In these tests, loose Sengenyama sand was used at a relative density of 40%. Sasaki *et al.* (1991, 1992) report a series of tests (Figs. 17-19) in which the liquefiable layer was a loose mountain sand (Mt. Sengen-yama sand) built by an underwater drop method. In these tests, the characteristics of dilative soil response are evident from the recorded acceleration spikes and the corresponding acc-lateral displacement response (Fig. 19b). Towhata and Toyota (1994) studied the response of a pipe in liquefied Toyoura sand and reported a similar response mechanism (Fig. 19c). Additional shake table tests were also conducted (Shamoto *et al.* 1996) using Toyoura sand at a relative density of 53% (Fig. 20). The reported results also demonstrate the above-described aspect of dilatant soil response (in the form of response acceleration spikes).

IN-SITU SEISMIC RESPONSE

The Wildlife Refuge (California, USA): This site is located on the West Side of the Alamo River in Imperial County, southern California. Evidence of liquefaction was observed at or near the site following the 1930, 1950, 1957, 1979, and 1981 Imperial Valley earthquakes (Youd and Wieczorek 1984). These observations triggered an interest in the site, which was instrumented in 1982, in an insightful effort (Youd and Wieczorek 1984) by the United States Geological Survey (USGS). In 1987, the site was shaken by two main earthquakes (Holzer *et al.* 1989), including the Superstition Hills earthquake (M_W = 6.6), which caused a sharp increase in recorded pore-water pressure. In addition, subsequent field investigations showed evidence of site liquefaction and ground fissures. The surface records displayed peculiar acceleration spikes (Holzer *et al.* 1989) associated with simultaneous instants of excess pore-pressure drop (Fig. 21).

Using the simple approach of Koga and Matsuo (1990), the site lateral seismic response during liquefaction was inferred from the stress-strain and effective-path histories (Figs. 22 and 23) of the Superstition Hills earthquake (Zeghal and Elgamal 1994). At low effective confining pressures (high excess pore pressures), the effective stress-path clearly exhibited a reversal of behavior from contractive to dilative (Fig. 22), as the line of phase transformation was approached (National Research Council 1985). Such a mechanism is a consequence of soil dilation at large strain excursions, resulting in associated instantaneous pore-pressure drops as documented by the laboratory tests (Fig. 22b) of Vucetic and Dobry (1988).

Aomori Harbor (Japan): Towhata *et al.* (1996) presented (Fig. 24) a ground surface lateral acceleration history recorded at Aomori Harbor during the 1968 Tokatchi-Oki earthquake. This history was recorded at a location where liquefaction of subsoil was observed. In fact, the Wildlife site acceleration record (Fig. 21) shows a pattern of spikes, which is quite similar to that of this Aomori Harbor record (Fig. 24). Thus, a shear stress-strain response of similar characteristics to that at Wildlife might have occurred at Aomori Harbor during this earthquake.

Port Island (Kobe, Japan): Port Island is an artificial (reclaimed) island located on the west-south side of Kobe, Japan. In the phase completed by 1981, 436 ha were reclaimed by bottom dumping from barges (Nakakita and Watanabe 1981). Soil (Fig. 13) in the artificial reclaimed layer (O'Rourke 1995, Sitar 1995, Soils and Foundations 1996) consisted of decomposed weathered granite fill (Masado soil mined from the nearby Rokko mountains) with grain sizes ranging from gravel and cobble-sized particles, to fine sand (2 mm mean particle size, with silt-sized particles or smaller of less than 10% by weight).

A downhole accelerometer array was installed at the Northwest corner of Port Island in August 1991(Iwasaki 1995). The array consisted of triaxial accelerometers located at the surface, 16 m, 32 m, and 83 m depths. This array documented the observed widespread liquefaction of reclaimed ground during the 1995 Hyogoken-Nambu earthquake. Using the recorded downhole accelerations, the corresponding one-dimensional shear stress-strain response was evaluated (Elgamal *et al.* 1995, 1996a). At shallow depths, the stress-strain histories indicated (Fig. 25): (1) a noticeable reduction in stiffness with slight but visible signs of shear strain hardening at elevation 24m, and (2) an abrupt sharp loss of stiffness and reduction of yield strength near the surface at 8m depth. It is noted here that no clear signs of permanent lateral deformations were observed at the array site.

Kushiro Port (Japan): Iai *et al.* (1995) presented downhole accelerations recorded during the 1993 Kushiro-oki earthquake. The downhole array is located in Kushiro port. Upper layers at this site included saturated sand with shear wave velocities of 250 m/sec. The recorded accelerations showed clear spikes at ground surface and at 2 m depth (Fig. 26). These spikes were attributed to sand dilation, and were successfully simulated by a noteworthy computational model (Fig. 27) as will be discussed below. In this case, acceleration spikes do not necessarily denote r_u values approaching or equal to 1.0, but may nevertheless be associated with significant increase in excess pore-water pressure.

CENTRIFUGE EXPERIMENTS

Lee and Schofield (1988) reported the occurrence of spiky acceleration response near the slopes of saturated model sand embankments (Figs. 28). The soil was Leighton Buzzard sand, which was in a dense state during this observed spiky response. The spikes were appropriately attributed to an underlying dilative mechanism as suggested qualitatively -for

instance- by the triaxial testing results (Fig. 6) of Tatsuoka (1972).

A large body of centrifuge experiments using Nevada Sand (Arulmoli *et al.* 1992, Taboada and Dobry 1992) has also shown clear evidence of cyclic dilative soil response effects. Many of these experiments are described in (Arulanandan and Scott 1993, 1994) as part of the VELACS project (Taboada and Dobry 1993, Scott *et al.* 1993, Wilson *et al.* 1993, Dobry and Taboada 1994, Whitman and Ting 1994). Relative density of the Nevada sand varied within the range of about 40% to 75% in these tests. A representative set of recorded accelerations is shown in Figs. 29-31. In addition to VELACS, a number of RPI Ph.D. theses contain extensive evidence of this response (e.g., Liu 1992, Taboada 1995, Adalier 1996, Abdoun 1997). A large number of studies (mostly using Nevada Sand) conducted at the University of California, Davis (e.g., Divis *et al.* 1996, Arulanandan *et al.* 1977, Balakrishnan et al. 1997, Wilson et al. 1997) also show a similar response (e.g., Fig. 32).

The basic nature of associated shear stress-strain response is clearly manifested by back-calculated shear stress-strain lateral-deformation histories as reported by Dobry *et al.* (1995) and Elgamal et al. (1996b). These histories (Fig. 33) are based on the recorded acceleration and displacement responses of infinite mild-slope dynamic simulations in a set of pioneering tests conducted by Taboada (1995), and duplicated by Scott et al. (1993).

COMPUTATIONAL MODELS

A number of computational models have become available recently to simulate the processes associated with sand dilation during liquefaction (Prevost 1985, Pastor and Zienkiewicz 1986, Matsuoka and Sakakibara (1987), Nishi and Kanatani 1990, Iai 1991, Anandarajah 1993, Aubry *et al.* 1993, Bardet *et al.* 1993, Byrne and McIntyre 1994, Proubet 1991, Li 1990, 1993, Kimura *et al.* 1993, Tobita and Yoshida 1995). The general response characteristics of these models may be inferred from Figures 34-39. Many of the essential features of cyclic mobility have been successfully modeled by (Iai 1991), under undrained loading conditions as shown by the computed acceleration during the 1993 Kushiro-oki earthquake (Fig. 27).

At this point, few results have been published to show the performance of these constitutive models for the important case of an acting driving shear stress (e.g., lateral spreading situation, near and below slopes, the retaining wall problem). Such situations demand a high degree of control over accumulated cycle by cycle deformations (Fig. 3) as depicted in Fig. 40 (Tateishi et al. 1995).

Recently, a simple displacement-controlled sliding-block approach was proposed to simulate the dilatant stick-slip process shown in Figs. 3 and 40b. This new simplified approach (Fig. 41) is described in Abdoun (1994), Abdoun and Elgamal (1995), and Taboada *et al.* (1996).

NEW CONSTITUTIVE MODEL

A new soil constitutive model was developed (Parra 1996), based on the original framework of plasticity theory for frictional cohesionless soils presented by Prevost (1985). The main purpose of this model is to simulate the characteristics of soil response described above, including the biased accumulation of cyclic shear strains due to the presence of a locked-in driving shear stress. A Biot-type theory for solid-fluid coupled analyses after the works of Chan (1988) and Zienkiewicz *et al.* (1990) was also numerically implemented for that purpose (Ragheb 1994, Parra 1996). This coupled formulation and the developed constitutive model were implemented in a general purpose 2-D (plane strain and axisymmetric) finite element program (see Appendix I). A typical response of this constitutive model is shown in Figs. 22a and 42. The model was developed and thoroughly calibrated by laboratory and centrifuge tests on Nevada Sand (Parra 1996). It was also calibrated and employed to simulate (Fig. 43) the recorded Port Island downhole array response during the 1995 Hyogo-ken Nambu, Kobe earthquake (Elgamal *et al.* 1996b).

SUMMARY AND CONCLUSIONS

During liquefaction (r_u approaching 1.0) of clean sands, the phenomenon of regain in shear strength at large shear-strain excursions (also known as a form of cyclic-mobility) may be of paramount importance in restricting the extent of shear lateral deformation due to seismic excitation. Consequently, constitutive models that capture this phenomenon are essential in analyses of such an important soil response mechanism. These models must reliably model the cycle-by-cycle biased accumulation of permanent deformations, especially in the presence of an imposed locked-in driving shear stress. Currently, further quantification of the underlying response mechanisms is underway through laboratory, shake-table, and centrifuge experiments (e.g., effects of extent of load reversal, number of load cycles, level of driving shear strength, and relative density of soil on magnitude of accumulated shear strain).

In this paper, a review of reported cyclic-mobility response was presented, as documented by experiments and case histories. Efforts towards computational simulation of this response were also surveyed.

Under conditions of an imposed driving shear stress, the tendency for soil dilation during liquefaction appears to have a dominant impact on the magnitude of seismically-induced accumulated shear deformations in clean sands (and possibly clean non-plastic silts). This applies to most situations of relative density encountered in practice (e.g., relative density D_r > 35%). In this regard, residual strength during

liquefaction (before the onset of dilation and associated regain in shear strength) may only play a relatively minor role. This residual strength on the other hand, might play a more significant role for sandy/silty soils with or without stratification (e.g., sands mixed with silts and clays). Research in this area is needed to clarify and quantify the associated deformation mechanisms in such commonly encountered natural and constructed soil formations.

ACKNOWLEDGMENTS

The research reported herein was supported by the United States Geological Survey (grant No. 1434-HQ-97-GR-03070), INTEVEP, SA, Venezuela, and the National Science Foundation (grant No. MSS-9057388). This support is gratefully acknowledged. The employed Port Island downhole acceleration data were provided by the Committee of Earthquake Observation and Research in the Kansai Area (CEORKA), Japan, with the help of Dr. Y. Iwasaki.

APPENDIX I

Description of New Computational Model

Soil was modeled as a two-phase material using the Biot (1962) formulation for porous media. This formulation was incorporated in a general purpose 2-D finite element program (Ragheb 1994, Parra 1996) using the u-p formulation (in which displacement of the soil skeleton, u, and pore pressures, p, are the unknowns) suggested by Zienkiewicz et *al.* (1990). The computational scheme follows the methodology of Chan (1988), which is based on the following assumptions: small deformations and rotations, density of the solid and fluid is constant in both time and space, porosity is locally homogeneous and constant with time, incompressibility of the soil grains, and equal accelerations for the solid and fluid phases.

Therefore, the general coupled formulation after the spatial discretization and Galerkin approximation is expressed as follows:

$$\mathbf{M}\ddot{\mathbf{u}} + \int_{\Omega} \mathbf{B}^T \boldsymbol{\sigma}' d\Omega - \mathbf{Q}\mathbf{p} - \mathbf{f}^s = \mathbf{0} \qquad (1a)$$

$$\mathbf{G}\ddot{\mathbf{u}} + \mathbf{Q}^T\dot{\mathbf{u}} + \mathbf{H}\mathbf{p} + \mathbf{S}\dot{\mathbf{p}} - \mathbf{f}^p = \mathbf{0} \qquad (1b)$$

Where **M** is the mass matrix, **B** is the strain-displacement matrix, $\boldsymbol{\sigma}'$ is the effective stress vector, **Q** is the discrete gradient operator coupling the solid and fluid phases, **u** is the displacement vector, **p** is the pore pressure vector, **G** is the dynamic seepage force matrix, **H** is the permeability matrix, **S** is the compressibility matrix, and $\mathbf{f}^s$ and $\mathbf{f}^p$ are the prescribed boundary conditions for solid and fluid phase respectively. A superposed dot denotes time derivative. Viscous damping is added for the solid phase in the form of Rayleigh damping ($\mathbf{C} = \alpha\mathbf{M} + \beta\mathbf{K}$), where **K** is the initial stiffness matrix). For earthquake loading problems, **G** is usually neglected so that symmetry of the global matrix is attained.

Equation 1 is integrated in time using a simple single step predictor multi-corrector scheme of the Newmark type (Katona and Zienkiewicz 1985), with an automatic time stepping split algorithm, incorporated to improve the rate of convergence. The predictor is calculated using the initial stiffness matrix method, as the high degree of non-associativity shown in the behavior of the solid phase for granular materials, produces a non-symmetric tangent stiffness matrix that requires a non-symmetric matrix solver. Experience based on analyses of non-associative plasticity shows that the initial stiffness method performs reasonably well (Chan 1988).

The second term in Eq. 1a is defined by the soil constitutive model. In this study, a new model is developed and used, based on the original work on plasticity theory for frictional cohesionless soils (Prevost 1985). The new model (Parra 1996) provides flexibility in modeling the cyclic mobility phenomenon. Special attention is given to the way the deviatoric-volumetric strain coupling occurs under cyclic loading, especially for loading-unloading-reloading situations above the phase transformation line, and near the liquefaction condition ($p' = 0$ condition).

The constitutive equation is written in incremental form as follows (Prevost 1985):

$$\dot{\boldsymbol{\sigma}} = \mathbf{E} : (\boldsymbol{\varepsilon} - \dot{\boldsymbol{\varepsilon}}^p) \qquad (2)$$

Where $\dot{\boldsymbol{\sigma}}$ is the rate of effective stress tensor, $\dot{\boldsymbol{\varepsilon}}$ is the rate of deformation tensor, $\dot{\boldsymbol{\varepsilon}}^p$ is the plastic rate of deformation tensor, and **E** is the isotropic elastic coefficient fourth order tensor. In this equation the superposed dot denotes a material derivative. The plastic rate of deformation tensor is defined by: $\dot{\boldsymbol{\varepsilon}}^p = \mathbf{P}\langle L \rangle$, where **P** is a symmetric second-order tensor which defines the direction of plastic deformation in stress, L is the plastic loading function; and the symbol $\langle\ \rangle$ denotes the McCauley's brackets (*viz.*, L=0 if L<0). Otherwise, L is defined as: $L = \mathbf{Q}:\dot{\boldsymbol{\sigma}} / H'$ where H' is the plastic modulus, and **Q** is a symmetric second-order tensor which defines, in stress space, the direction of the outer normal to the yield surface ($\mathbf{Q} = \nabla f / \|\nabla f\|$).

The yield function, f, representing the states of stress for which plastic flow occurs, is selected as a family of nested cone surfaces connected at the apex as follows (Lacy 1986):

$$f = \frac{3}{2}(\mathbf{s} - p\boldsymbol{\alpha}) : (\mathbf{s} - p\boldsymbol{\alpha}) - m^2 p^2 = 0$$

where $\mathbf{s} = \boldsymbol{\sigma} - p\boldsymbol{\delta}$ is the deviatoric stress tensor, $p = p - a$ with p and a representing the effective mean normal stress and the attraction at the apex (given by the amount of residual shear strength) respectively, α is the kinematic deviatoric tensor

defining the coordinates of the yield surface, and m is a material parameter to describe the friction angle ϕ .

The flow rule is chosen so that the deviatoric component of flow $\mathbf{P}' = \mathbf{Q}'$ (associative flow rule in the deviatoric plane), and the volumetric component $P^{\bullet}$ gives the desired amount of dilation or contraction in accordance with laboratory or field observations. Consequently, $P^{\bullet}$ defines the degree of non-associativity of the flow rule and is given as follows (Parra 1996):

$$3P^{\bullet} = \frac{(\eta/\overline{\eta})^2 - 1}{(\eta/\overline{\eta})^2 + 1} \Psi_d \langle \xi_d \rangle$$

Where $\eta = ((3/2)\mathbf{s} : \mathbf{s})^{1/2}/p$ is effective stress ratio, $\overline{\eta}$ is a material parameter defining the stress ratio at the phase transformation (PT) line, Ψ_d is a dilation function scaling the amount of dilation or contraction depending on the level of confining pressure and cumulative plastic deformation, and $\xi_d = f(\varepsilon_d^v - \varepsilon_y^p)$ is an effective dilation function triggered at the point when the cumulative plastic deformation in the dilative zone ε_d^v reaches a predefined yielding level ε_y^p. The sign of $(\eta/\overline{\eta})^2 - 1$ dictates dilation or contraction. If negative, the stress point lies below the PT line and contraction takes place. On the other hand, when the sign is positive the stress point lies above the PT line and dilation occurs. However, contrary to the original Prevost (1985) formulation, contraction above the PT line is performed towards the point where dilation started, which acts as a memory for the dilation-contraction condition. At the point of initial liquefaction or $p' = 0$ only dilation is allowed and upon contraction $P^{\bullet}$ is set equal to zero.

A purely deviatoric kinematic rule is chosen according to: $p\dot{\boldsymbol{\alpha}} = b\boldsymbol{\mu}$, Where $\boldsymbol{\mu}$ is a deviatoric tensor defining the direction of translation (Lacy 1986) and b is the amount of translation dictated by the consistency condition.

The integration of the constitutive equations is performed using a stress point algorithm based upon the radial return method in the deviatoric plane (Lacy 1986), with an automatic strain stepping split algorithm, which guarantees convergence and accuracy at all levels of strain (Parra 1996).

REFERENCES

Abdoun, T. [1994]. "Prediction of Soil Deformation Due to Seismically Induced Liquefaction," MS Thesis, Dept. of Civil Engineering, Rensselaer Polytechnic Institute, Troy, NY.

Abdoun, T. and Elgamal, A. -W. [1995]. "Prediction of Seismically-Induced Lateral Deformation During Soil Liquefaction," Eleventh African Regional Conference on Soil Mechanics and Foundation Engineering, International Society for Soil Mechanics and Foundation Engineering, Cairo, Egypt, Dec. 11-15, 1995.

Abdoun, T. [1997]. "Modeling of Seismically Induced Lateral Spreading of Multi-Layered Soil and Its Effect on Pile Foundations," Ph.D. Thesis, Department of Civil Engineering, Rensselaer Polytechnic Institute, Troy, NY.

Adalier, K. [1996]. "Mitigation of Earthquake Induced Liquefaction Hazards," Ph.D. Thesis, Department of Civil Engineering, Rensselaer Polytechnic Institute, Troy, NY.

Anandarajah [1993]. "VELACS project: Elasto-Plastic Finite Element Predictions of the Liquefaction Behavior of Centrifuge Models Nos 1, 3 and 4a," Proc. of the Intl. Conference on the Verification of Numerical Procedures for the Analysis of Soil Liquefaction Problems, Arulanandan, K. and Scott, R. F., Eds. Vol. 1, Davis, CA, 45-66, Balkema.

Arulanandan, K. and Scott, R. F., Eds. [1993]. *Verification of Numerical Procedures for the Analysis of Soil Liquefaction Problems*, Conference Proceedings, Davis, CA, Volume 1, Balkema.

Arulanandan, K. and Scott, R. F., Eds. [1994]. *Verification of Numerical Procedures for the Analysis of Soil Liquefaction Problems*, Conference Proceedings, Davis, CA, Volume 2, Balkema.

Arulanandan, K., Muraleetharan, K. K., Yogachandran, C., [1997]. "Seismic Response Of Soil Deposits In San Francisco Marina District," Journal of Geotechnical and Geoenvironmental Engng., ASCE, 123, 10, Oct., 965-974.

Arulmoli, K., Muraleetharan, K. K., Hossain, M. M., and Fruth, L. S. [1992]. "*VELACS: Verification of Liquefaction Analyses by Centrifuge Studies, Laboratory Testing Program, Soil Data Report*," Report, The Earth Technology Corporation, Project No. 90-0562, Irvine, California.

Aubry, D., Benzenati, I. and Modaressi, A. [1993]. "Numerical Predictions for Model No. 1," Proc. of the Intl. Conference on the Verification of Numerical Procedures for the Analysis of Soil Liquefaction Problems, Arulanandan, K. and Scott, R. F., Eds. Vol. 1, Davis, CA, 45-66, Balkema.

Balakrishnan, A., Kutter, B. L. and Idriss, I. M. [1997]. "Liquefaction Remediation at Bridge Sites- Centrifuge data Report For BAM05," Report No. UCD/CGMDR-97/10, Center for Geotechnical Modeling, Department of Civil and Environmental Engng, University of California, Davis, May.

Bardet, J.P., Huang, Q. and Chi, S. W. [1993]. "Numerical Prediction for Model No. 1," Proc. of the Intl. Conference on the Verification of Numerical Procedures for the Analysis of Soil Liquefaction Problems, Arulanandan, K. and Scott, R. F., Eds. Vol. 1, Davis, CA, 67-86, Balkema.

Biot, M. A. [1962]. "The Mechanics of Deformation and Acoustic Propagation in Porous Media," J. Appl. Phys., 33, 4, 1482-1498.

Byrne, P. M. and McIntyre, J. [1994]. "Deformations in Granular Soils due to Cyclic Loading," Proceedings of Settlement 94, ASCE Geotechnical Special Publication No. 40, Texas, June, pp. 1864-1896.

Casagrande, A. [1975]. "Liquefaction and Cyclic Deformation of Sands - A critical Review," Proceedings, 5th Pan-American Conference on Soil Mechanics and Foundation Engineering, Buenos Aires, Argentina; also published as Harvard Soil Mechanics Series No. 88, January 1976, Cambridge, Mass.

Castro, G. [1975]. Liquefaction and Cyclic Mobility of Saturated Sands. Journal of the Geotechnical Engineering Division, ASCE, 101, GT6, 551-569.

Castro, G and Poulos, S. J. [1977]. "Factors Affecting Liquefaction and Cyclic Mobility," Journal of the Geotechnical Engineering Division, ASCE, Vol. 103, No. GT6, June, pp. 501-516.

Chan, A. H. C. [1988]. A Unified Finite Element Solution to Static and Dynamic Problems in Geomechanics. Ph.D. dissertation, University College of Swansea, U. K.

Dobry, R. and Taboada, V. M. [1994]. "Possible Lessons from VELACS Model No. 2 Results," Proc. of the International Conference on the Verification of Numerical Procedures for the Analysis of Soil Liquefaction Problems, Arulanandan, K. and Scott, R. F., Eds. Vol. 2, Davis, CA, 1341-1352, Balkema.

Dobry, R., Taboada, V. and Liu, L. [1995]. "Centrifuge Modeling of Liquefaction Effects During Earthquakes," Proc. 1st Intl. Conf. On Earthquake Geotechnical Engineering (IS-Tokyo), Keynote Lecture, Ishihara, K. Ed., 3, Balkema, Nov. 14-16, Tokyo, Japan, 1291-1324.

Divis, C. J., Kutter, B. L., and Idriss, I. M. [1996]. "Uniformity of Specimen and Response of Liquefiable Sand Model In A Large Centrifuge Shaker," Proc. 6th U.S.-Japan Workshop on Earthquake Resistant Design of Lifeline Facilities and Countermeasures Against Liquefaction," June 11-13, Waseda University, NCEER Report, Buffalo, NY.

Elgamal, A. -W., Zeghal, M., and Parra, E. [1995]. "Identification and Modeling of Earthquake Ground Response," Proc. 1st Intl. Conf. On Earthquake Geotechnical Engineering (IS-Tokyo), Special, Keynote and Theme Lectures Volume, Nov. 14-16, Tokyo, Japan.

Elgamal, A. -W., Zeghal, M., and Parra, E. [1996a]. "Liquefaction of Reclaimed Island in Kobe, Japan," J. Geotech. Engineering, ASCE, 122, 1, Jan., 39-49.

Elgamal, A. -W., Zeghal, M., Taboada, V. M. and Dobry, R. [1996b]. "Analysis of Site Liquefaction and Lateral Spreading using Centrifuge Model Tests," Soils and Foundations, 36, 2, June, 111-121.

Hatanaka, M., Uchida, A. and Ohara, J. [1997]. "Liquefaction Characteristics Of A Gravelly Fill Liquefied During The 1995 Hyogo-Ken Nanbu Earthquake," Soils and Foundations, 37, 3, 107-115.

Holzer, T. L., Youd T. L. and Hanks T. C. [1989]. "Dynamics Of Liquefaction During the 1987 Superstition Hills, California, Earthquake," Science, Vol. 244, 56-59.

Hyodo, M., Murata, H., Yasufuku, N. and Fujii, T. [1991]. "Undrained Cyclic Shear Strength And Residual Shear Strain of Saturated Sand By Cyclic triaxial tests," Soils and Foundations, 31, 3, Sept., 60-76.

Iai, S. [1991]. "A Strain Space Multiple Mechanism Model for Cyclic Behavior of Sand and its Application," Earthquake Engineering Research Note No. 43, Port and Harbor Research Institute, Ministry of Transport, Japan.

Iai, S., Morita, T., Kameoka, T., Matsunaga, Y. and Abiko, K. [1995]. "Response of a Dense Sand Deposit During 1993 Kushiro-Oki Earthquake," Soils and Foundations, 35, 1, March, 115-131.

Ishihara, K. [1985]. "Stability of Natural Deposits During Earthquakes," Theme Lecture, Proceedings, 11th International Conference on Soil Mechanics and Foundation Engineering, San Francisco, Vol. 2, 321-376.

Ishihara, K., Verdugo, R., Acacio, A. [1991]. "Characterization of Cyclic Behavior of Sand and Post-Seismic Stability Analyses," Proc. IX Asian Regional Conference on Soil Mech and Found Eng, Bangkok, Thailand.

Iwasaki, Y. [1995]. "Geological and Geotechnical Characteristics of Kobe Area and Strong Ground Motion Records by 1995 Kobe Earthquake, Tsuchi-to-Kiso," Japanese Society of Soil Mechanics and Foundation Engineering, Vol. 43, No. 6, 15-20 (in Japanese).

Katona, M. G. and Zienkiewicz, O. C. [1985]. A Unified Set of Single Step Algorithms. Part 3: The Beta-m Method, A Generalization of the Newmark Scheme, Int. J. Num. Meth. Engng., 21, 1345-1359.

Kawakami, T., Suemasa, N., Hamada, M., Sato, H. and Kotada, T. [1994]. "Experimental Study on Mechanical Properties of Liquefied Sand," Proc. 5th U.S.-Japan Workshop on Earthquake Resistant Design of Lifeline Facilities and Countermeasures Against Soil Liquefaction," T.D. O'Rourke and M. Hamada, Eds., Snowbird, Utah, Report NCEER-94-0026, Buffalo, NY, 285-299.

Koga, Y. and Matsuo, O. [1990]. "Shaking table tests of Embankments Resting on Liquefiable Sandy Ground," Soils and Foundations, 30, 4, 162-174.

Kimura, T., Takemura, J. and Hirooka, A. [1993]. "Numerical Prediction for Model No. 1," Proc. of the Intl. Conference on the Verification of Numerical Procedures for the Analysis of Soil Liquefaction Problems, Arulanandan, K. and Scott, R. F., Eds. Vol. 1, Davis, CA, 141-152, Balkema.

Lambe, T. W. and Whitman, R. V. [1969]. *"Soil Mechanics,"* John Wiley & Sons, New York.

Lacy, S. [1986]. "Numerical Procedures for Nonlinear Transient Analysis of Two-phase Soil System." Ph.D. dissertation, Princeton University, NJ, U.S.A.

Lee, F. H. and Schofield, A. N. [1988]. "Centrifuge Modelling of Sand Embankments and Islands in Earthquakes," Geotechnique, 38, No. 1, 45-58.

Li, X. S. [1990]. "Free Field Response under Multi-directional Earthquake Loading," Ph.D. Dissertation, Dept. of Civil Engng, University of California, Davis.

Li, X.S. [1993]. "Numerical Prediction for Model No. 1," Proc. of the Intl. Conf on the Verification of Numerical Proc for the Analysis of Soil Liquefaction Problems, Arulanandan, K. and Scott, R. F., Eds.1, Davis, CA, 169-178, Balkema.

Liu, L. [1992]. "Centrifuge Earthquake Modeling of Liquefaction and Its Effects on Shallow Foundations," Ph.D. Thesis, Dept of Civil Engineering, Rensselaer Polytechnic Institute, Troy, NY.

Matsuoka H. and Sakakibara A. [1987]. "A Constitutive Model for Sands and Clays Evaluating Principal Stress Rotation," Soils and Foundations, 27, 4, 73-88.

Nakakita, Y., and Watanabe, Y. [1981]. "Soil stabilization by Preloading in Kobe Port Island," Proceedings of the 9th International Conference on Soil Mechanics and Foundation Engineering, Tokyo, Japan, 611-622.

National Research Council [1985]. *"Liquefaction of Soils During Earthquakes,"* Committee on Earthquake Engineering, National Academy Press, Washington, D. C.

Nishi, K. and Kanatani, M. [1990]. "Constitutive Relations for Sand Under Cyclic Loading based On Elasto-Plasticity Theory," Soils and Foundations, 30, 2, 43-59.

O'Rourke, T. D. [1995]. "Geotechnical Effects," Preliminary Report from the Hyogoken-Nanbu Earthquake of January 17, 1995, National Center for Earthquake Engineering Research Bulletin, SUNY, Buffalo, Vol. 9, No. 1.

Parra, E. [1996]. "Numerical Modeling of Liquefaction and Lateral Ground Deformation Including Cyclic Mobility and Dilation Response in Soil System," Ph.D. Thesis, Dept. of Civil Engineering, Rensselaer Polytechnic Institute, Troy, NY.

Pastor, M. and Zienkiewicz, O. C. [1986]. "A Generalized Plasticity Hierarchical Model for Sand under Monotonic and Cyclic Loading," Proceedings, 2nd International Conference on Numerical Models in Geomechanics, Pande G. N., and Van Impe W. F. (Eds.), M. Jackson and Son Publ., pp. 131-150.

Prevost, J. H., [1985]. "A Simple Plasticity Theory for Frictional Cohesionless Soils," Soil Dyn. And Earthquake Engineering, 4, 1, 9-17.

Proubet, J. [1991]. "Application of Computational Geomechanics to Description of Soil Behavior, Ph.D. dissertation, U. of Southern California, L A, California.

Ragheb, A. [1994]. "Numerical analysis of Seismically Induced Deformations in Saturated Granular Soil Strata," Ph.D. Thesis, Dept of Civil Engng, RPI, Troy, NY.

Sasaki, Y., Tokida, K., Matsumoto, H. and Saya, S. [1991]. "Experimental Study on Lateral Flow of Ground Due to Soil Liquefaction," Proc. 2nd Intl. Conf. On Recent Advances in Geotechnical Earthquake Engineering and Soil Dynamics, March 11-15, St. Louis, Missouri, Paper No. 2.22, 263-270.

Sasaki, Y., Towhata, I, Tokida, K., Yamada, K., Matsumoto, H., Tamari, Y. and Saya, S. [1992]. "Mechanism of Permanent Displacement of Ground Caused By Seismic Liquefaction," Soils and Foundations, 32, 3, Sept., 79-96.

Scott, R. F., Hushmand, B. and Rashidi, H. [1993]. "Duplicate Test of Model No 2: Sloping Loose Sand layer," Intl. Conf. on Verification of Num. Proc. for Anal. Of Soil Liquefaction Problems, Arulanandan, K. and Scott, R. F., Eds., 1, Davis, CA, 301-314, Balkema.

Scott, R. F. (1997). "Crane Response in 1995 Hyogoken Nanbu Earthquake," Soils and Foundations, 37, 2, 81-87, June.

Seed, H. B. and Lee, K. L. [1966]. "Liquefaction of Saturated Sands During Cyclic Loading," Journal of the Soil Mechanics and Foundations Division, ASCE, 92, SM6, Nov., 105--134.

Seed, H. B. [1979]. "Soil Liquefaction and Cyclic Mobility Evaluation for Level Ground During Earthquakes," J of the Geotech Engng Div, ASCE, 105, No. GT2, Feb., 201-255.

Shamoto, Y., Sato, M. and Zhang, J-M. [1996]. "Simplified Estimation of Earthquake-Induced Settlements In Saturated Sand Deposits," Soils and Foundations, 36, 1, March, 39-50.

Shamoto, Y., Zhang, J. -M., and Goto, S. [1997]. "Mechanism of Large Post Liquefaction Deformation in Saturated Sand," Soils and Foundations, 37, 2, June, 71-80.

Sitar, N., Ed. [1995]. "Geotechnical Reconnaissance of the Effects of the January 17, 1995, Hyogoken-Nanbu Earthquake

Japan," Report No. UCB/EERC-95/01, Earthquake Engineering Research Center, Berkeley, California.

Soils and Foundations [1996]. "Special Issue on Geotechnical aspects of the January 17, 1995 Hyogoken Nambu Earthquake," Soils and Foundations, Japanese Geotechnical Soc., January.

Taboada and Dobry [1992]. "Comparison Tests for Earth Technology's Laboratory tests, Report, Civil Engineering Department, Rensselaer Polytechnic Institute, Troy, NY.

Taboada, V. M. and Dobry, R. [1993]. "Experimental Results of Model 1 at RPI," Proc. Intl Conf Verification of Num. Proc. for the Analysis of Soil Liquefaction Problems, Arulanandan, K. and Scott, R. F., Eds., Volume 1, Davis, CA, 277-294, Balkema.

Taboada, V. M. [1995]. "Centrifuge Modeling of Earthquake-Induced Lateral Spreading in Sand Using a Laminar Box," Ph.D. Thesis, Rensselaer Polytechnic Institute, Troy, NY.

Taboada, V. M., Abdoun, T., and Dobry, R. [1996]. "Prediction of Liquefaction Induced Lateral Spreading by Dilatant Sliding Block Model Calibrated by Centrifuge Tests," Proc. 11WCEE, Acapulco, Mexico, June, Paper No. 376.

Tateishi, A., Taguchi, Y, Oka, F. and Yashima, A. [1995]. "A Cyclic Elasto-Plastic Model For Sand and Its Application Under various Stress Conditions," Proc. 1st Intl. Conf. On Earthquake Geotech Engng, 1, 399-404, Balkema, Rotterdam.

Tatsuoka, F. [1972]. "Shear Tests in a Triaxial Apparatus-a Fundamental Study of the Deformation of Sand (in Japanese), Thesis, Tokyo University.

Tatsuoka, F., Toki, S., Miura, S., Kato, H., Okamoto, M., Yamada, S., Yasuda, S., and Tanizawa, F. [1986]. "Some factors Affecting Cyclic Undrained Triaxial Strength of Sand," Soils and Foundations, 26, 3, Sept., 99-116.

Tobita, Y. and Yoshida, N. [1995]. "Stability of Mechanically Well-Behaved Constitutive Model in Liquefaction Analysis of Saturated Sands," Proc. 1st Intl. Conf. On Earthquake Geotechnical Engineering, Tokyo, Japan, 1, 429-434, Balkema.

Towhata, I. and Toyota, H. [1994]. "Dynamic Analysis of Lateral Flow of Liquefied Ground," 5th US-Japan Workshop on Earthquake Resist. Design of Lifeline Facilities and Countermeasures Against Soil Liquefaction," O'Rourke, T. D. and Hamada, M., Eds., Snowbird, Utah, Rep. NCEER-94-0026, Buffalo, NY, Nov.

Towhata, I, Park, J. K., and Orense, R. P. [1996]. "Use of Spectrum Intensity For Immediate Detection of Subsoil Liquefaction," Soils and Foundations, 36, 2, June, 29-44.

Vucetic, M. and Dobry, R. [1988]. "Cyclic Triaxial Strain-Controlled Testing of Liquefiable Sands," ASTM Spec. Tech. Publ. 977, Philadelphia, PA, 475-485.

Whitman, R. V. and Ting, Nai-Hsin [1994]. "Experimental Results For Tilting Wall With Saturated Backfill," Intl. Conf. Verification of Num. Proc. for Analysis of Soil Liquefaction Problems, Arulanandan, K. and Scott, R. F., Eds., 2, Davis, CA, 1515-1528, Balkema.

Wilson, D. and Kutter, B. L. [1993]. "Experimental Results of Model No. 7," Intl. Conf Verification of Num. Procedures for the Analysis of Soil Liquefaction Problems, Arulanandan, K. and Scott, R. F., Eds., 1, Davis, CA, 809-816, Balkema.

Wilson, D. W., Boulanger, R. W. and Kutter, B. L. [1997]. "Soil-Pile-Superstructure Interaction at Soft or Liquefiable Soils Sites-Centrifuge Data Report CSP3," Report No. UCD/CGMDR-97/04, Center for Geotech. Modeling, Dept. of Civil and Environ. Engineering, Univ. of California, Davis, February.

Yamashita, S., Toki, S., and Miura, K. [1989]. "Cyclic Undrained Triaxial and Torsional Shear Strength of Sand With Consideration of Membrane Penetration," Proc. 24th Annual Meeting on SMFE, Tokyo, 777-780 (in Japanese).

Yoshimi, Y. and Oh-oka, H. [1975]. "Influence of Degree of Shear Stress Reversal on the Liquefaction Potential of Saturated Sand," Soils and Foundations, 15, 3, 27-40.

Youd, T. L. [1977]. "Packing Changes and Liquefaction Susceptibility," Journal of the Geotechnical Engineering Division, ASCE, Vol. 103, GT8, August, 918-923.

Youd, T. L. and Wieczorek, G. F. [1984]. "Liquefaction During 1981 and Previous Earthquakes Near Westmorland California," U.S. Geological Survey Open-File Report 84-680.

Zeghal, M. and Elgamal, A. -W. [1994]. "Analysis of Site Liquefaction Using Earthquake Records," Journal of Geotechnical Engineering, ASCE, 120, No. 6, 996-1017.

Zhang, J. -M., Shamoto, Y. and Tokimatsu, K. [1997]. "Moving Critical and Phase Transformation Stress State Lines Of Saturated Sand During Undrained cyclic Shear," Soils and Foundations, 37, 2, June, 51-59.

Zienkiewicz, O. C., Chan, A. H. C., Pastor, M., Paul, D. K., and Shiomi, T. [1990]. "Static and Dynamic Behavior of Soils: A Rational Approach to Quantitative Solutions: I. Fully Saturated Problems," R. Soc. London, A 429, 285-309.

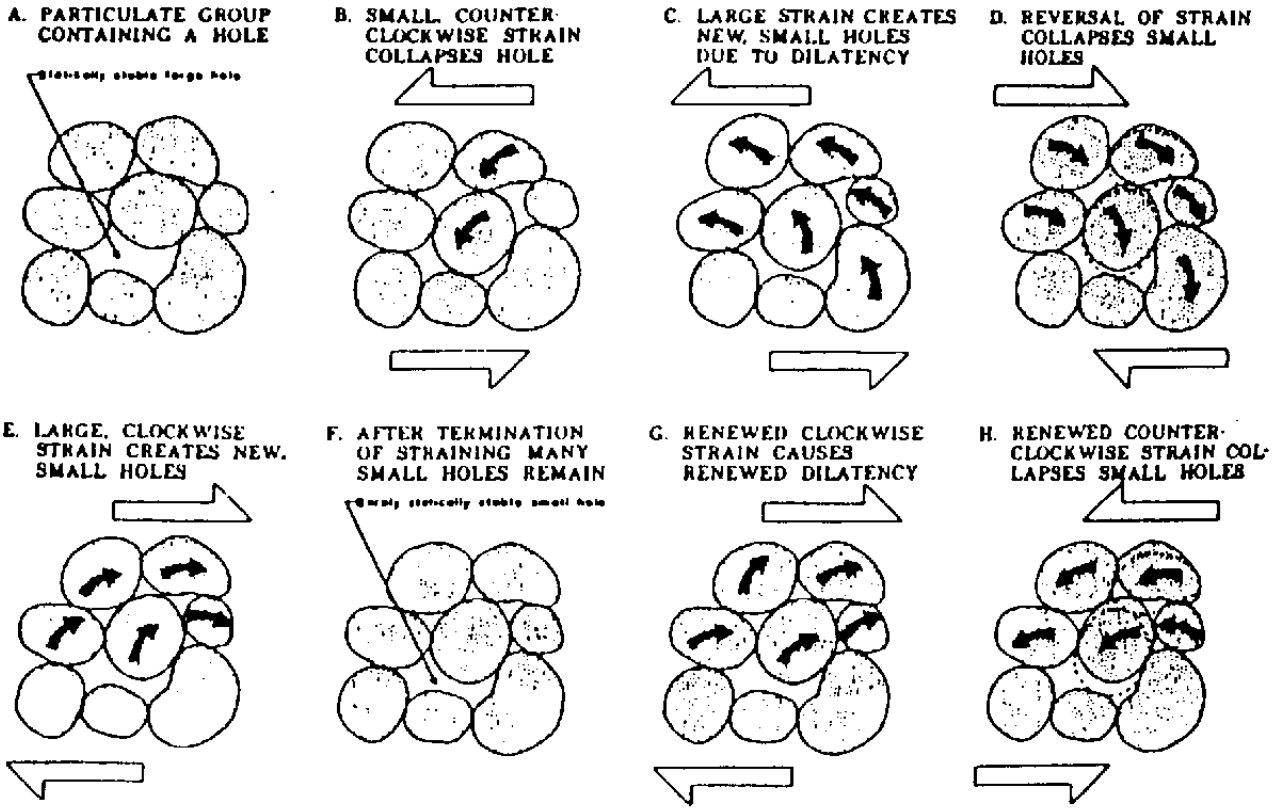

Figure 1. Diagrammatic cross section of particulate group showing packing changes that occur during cyclic loading (Youd 1977).

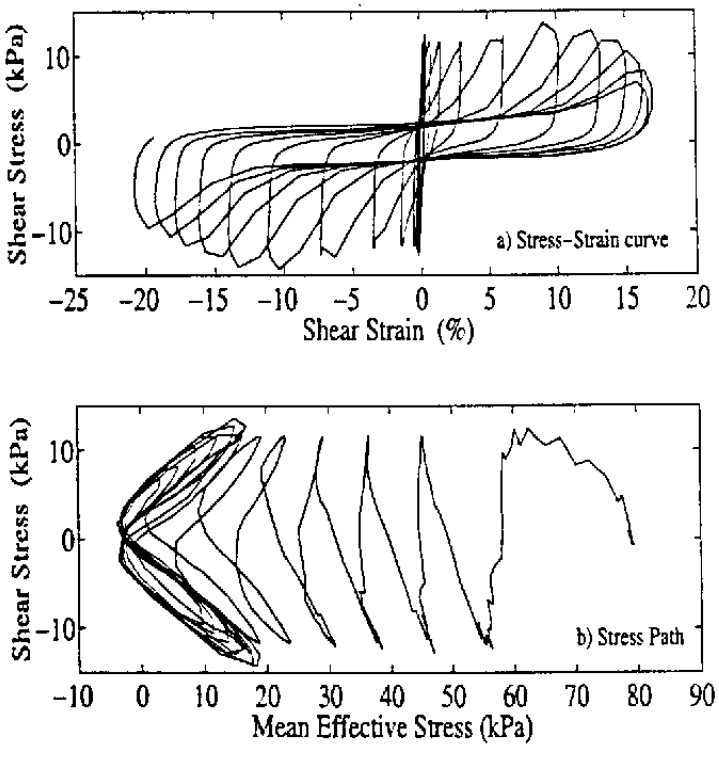

Figure 2. Stress-strain curve and stress-path for Nevada Sand with D_r=60% obtained from undrained cyclic simple shear (CSS) test (Arulmoli *et al.* 1992).

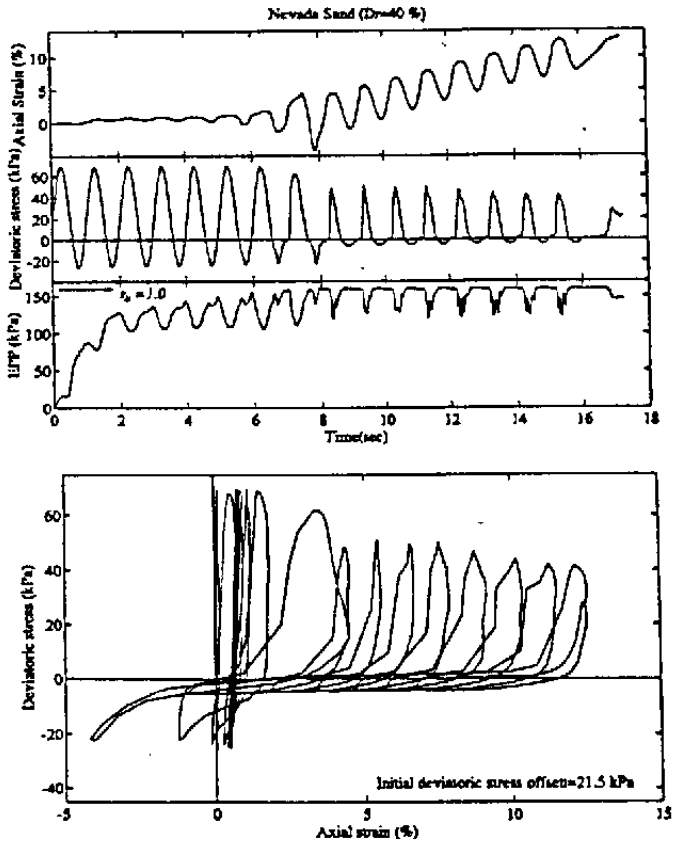

Figure 3a. Stress-strain and excess-pore-pressure histories during an undrained stress-controlled cyclic triaxial test of Nevada Sand (D_r=40%) with an imposed static (initial) deviatoric stress (Arulmoli *et al.* 1992).

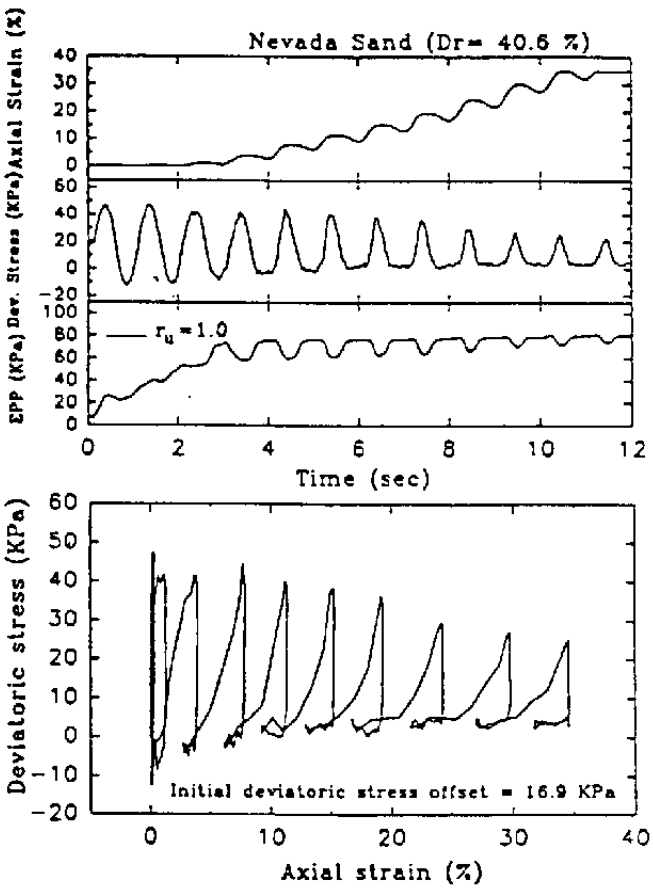

Figure 3b. Stress, strain and excess pore pressure histories during an undrained stress-controlled cyclic triaxial test of Nevada sand (Dr = 39.1%) with an imposed static (initial) deviatoric stress (Taboada and Dobry, 1992).

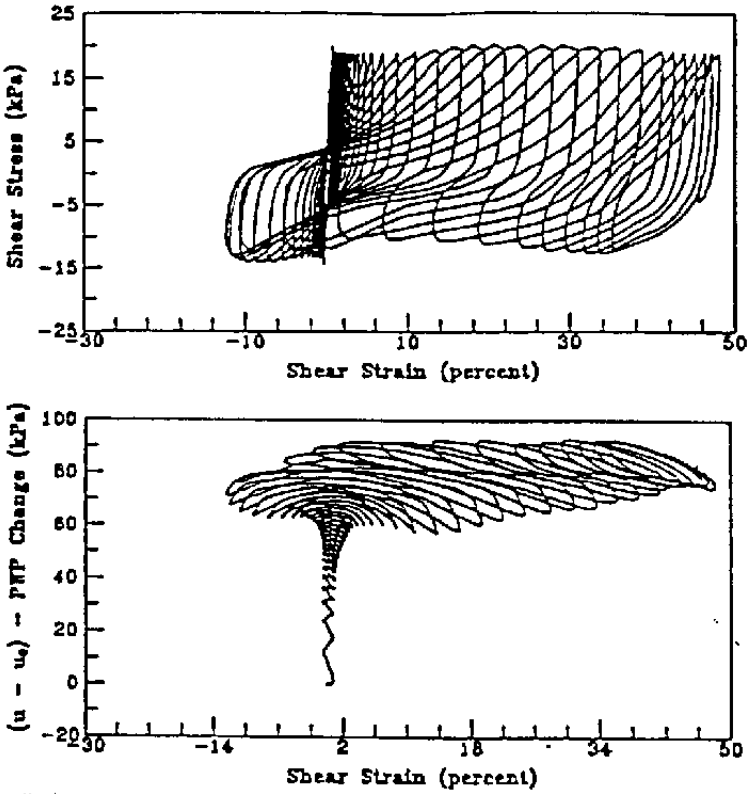

Figure 3c. Stress, strain and excess pore pressure histories during an undrained stress-controlled cyclic triaxial test of Bonnie silt with an imposed static (initial) deviatoric stress (Arulmoli et al. 1992).

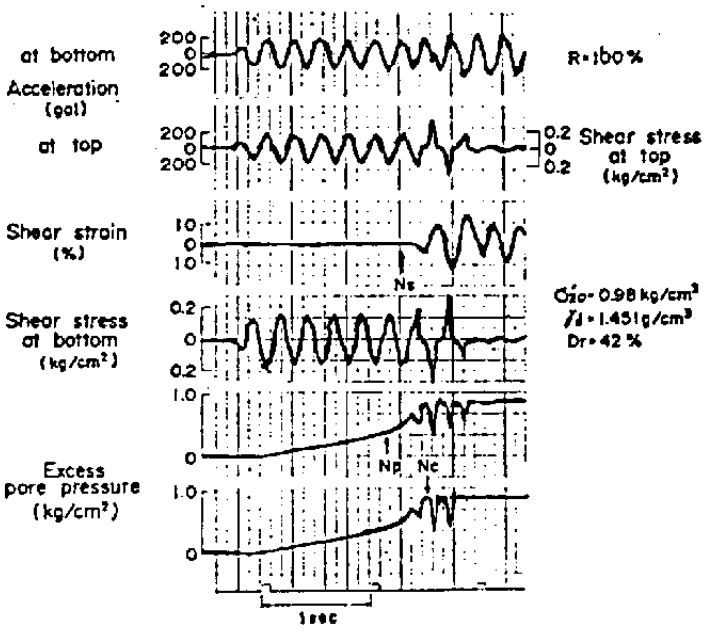

Figure 4a. Typical oscillograph records for the completely reversed shear tests (Yoshimi and Oh-oka 1975).

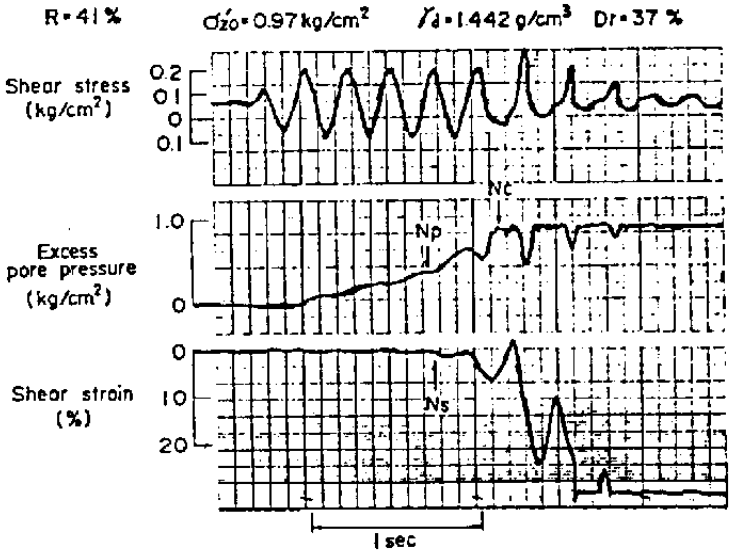

Figure 4b. Typical oscillograph records for the partially reversed shear tests (Yoshimi and Oh-oka 1975).

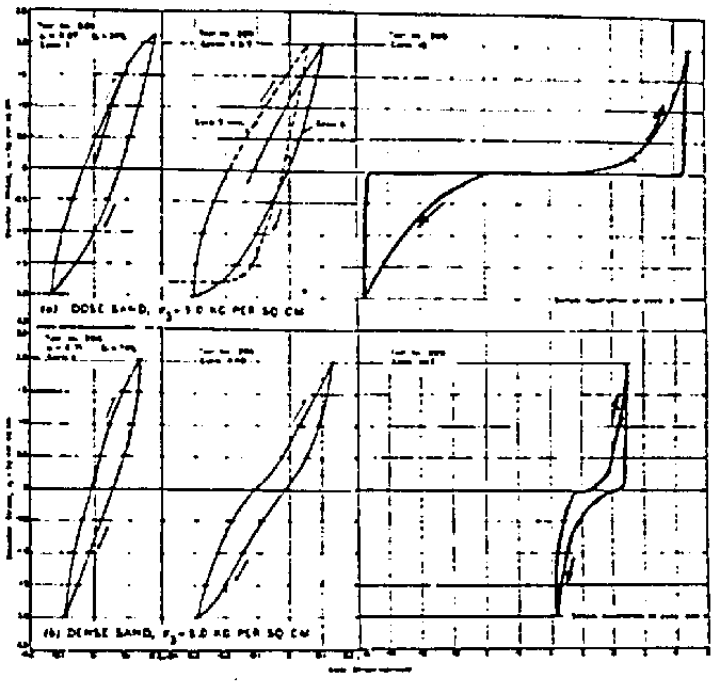

Figure 5. Hysteresis curves for cyclic loading test on Sacramento River Sand (Seed and Lee 1966).

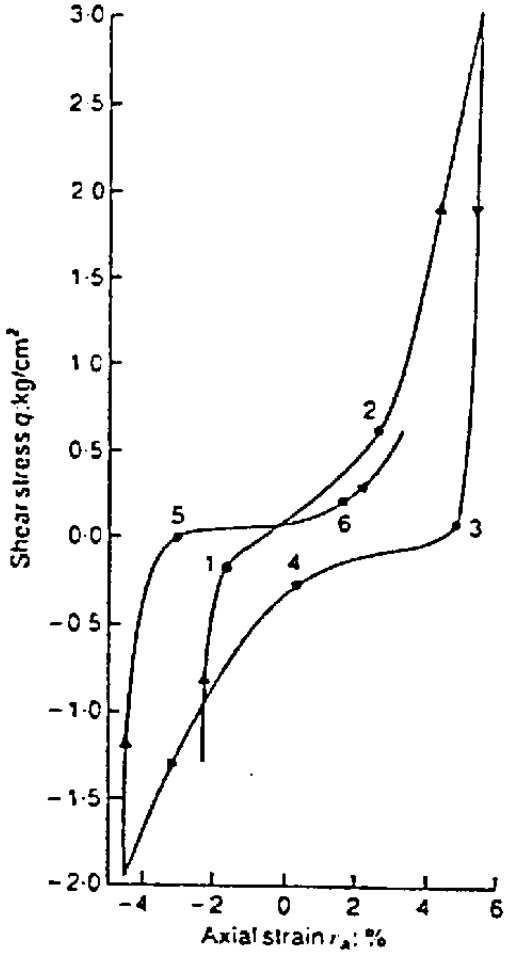

Figure 6. Variation in shear stress with axial strain reported by Tatsuoka 1972 (after Lee and Schofiled 1988).

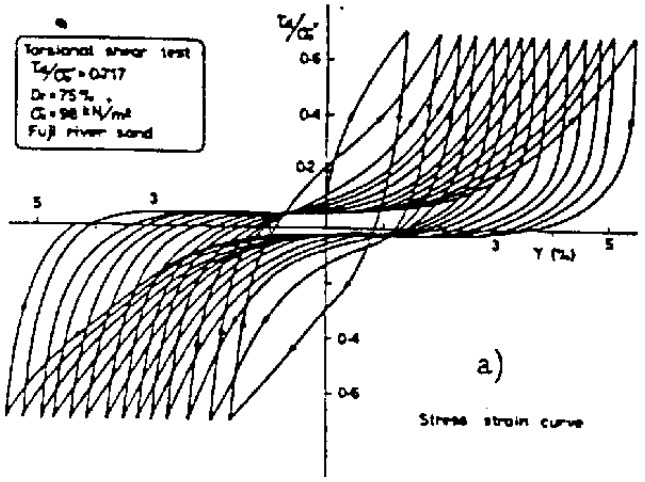

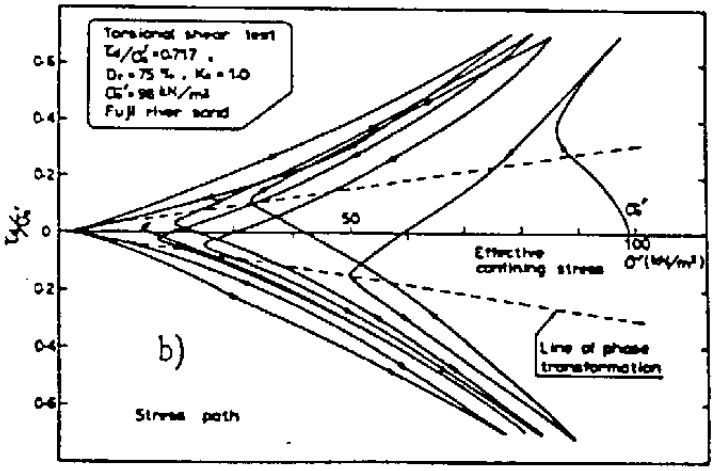

Figure 7. Stress-strain curve and stress path in cyclic torsional test on dense sand (Ishihara 1985).

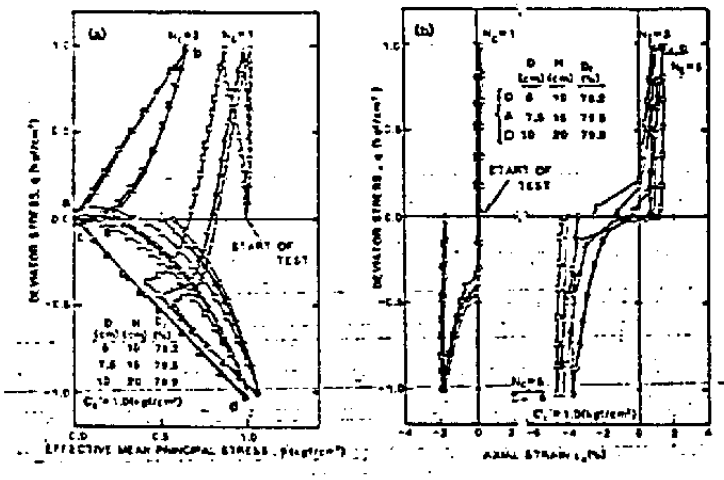

Figure 8a. Stress path and stress-strain hysteresis loop in tests by H. Kato (Tatsuoka *et al.* 1986).

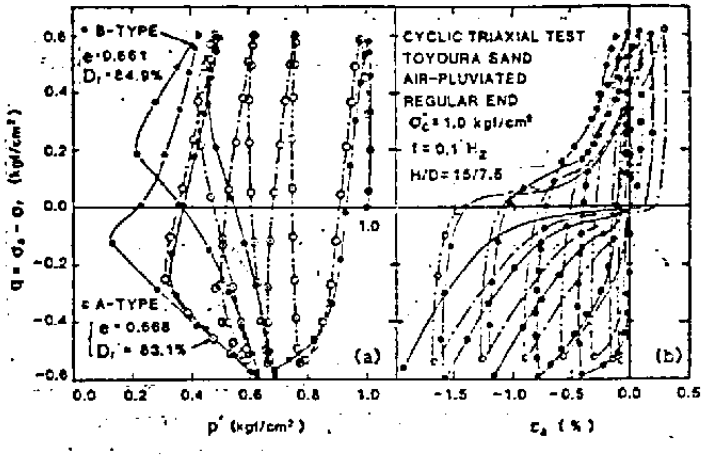

Figure 8b. Stress path and stress-strain hysteresis loop in tests by M. Okamoto, T. Torii and Y Yamada (Tatsuoka *et al.* 1986).

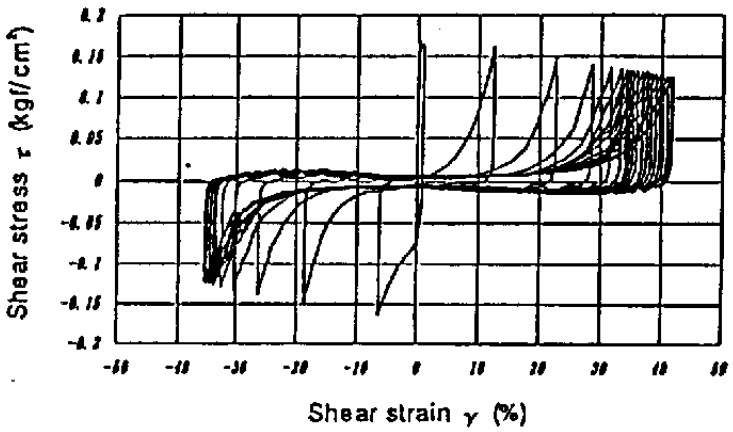

Figure 10. Relationship between shear stress and shear strain (Dr=53%, τ/σ_o'=0.2, σ_o'=1.0kgf/cm^2, f=0.1Hz (Kawakami *et al.* 1994).

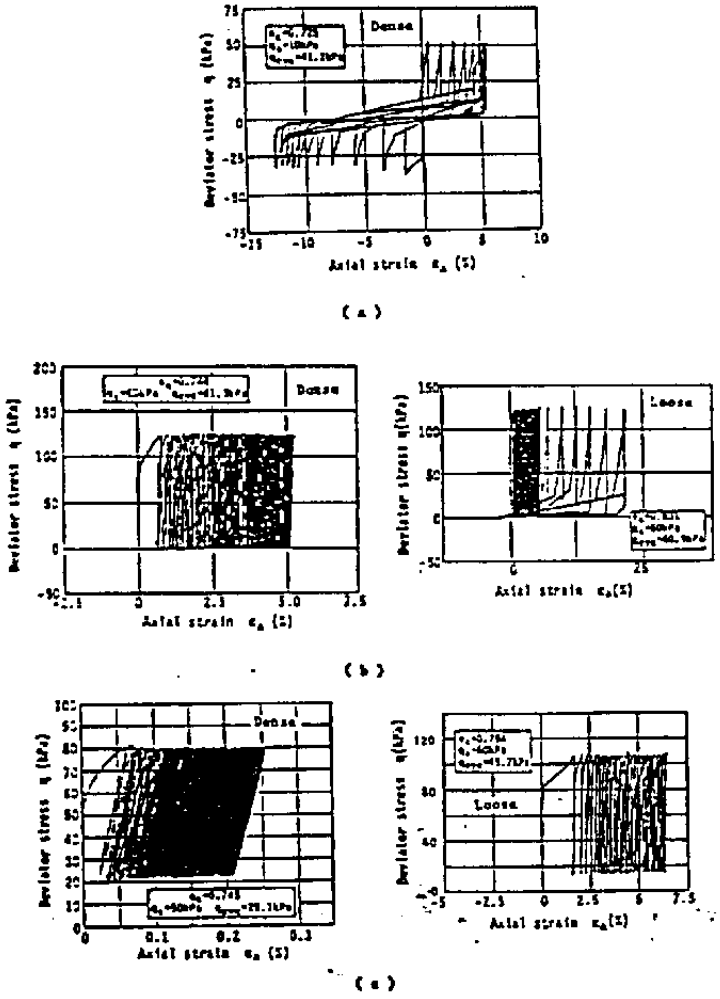

Figure 9. Relationship between deviatoric stress and axial strain, a) reversal, b) Intermediate, c) no reversal (Hyodo *et al.* 1991).

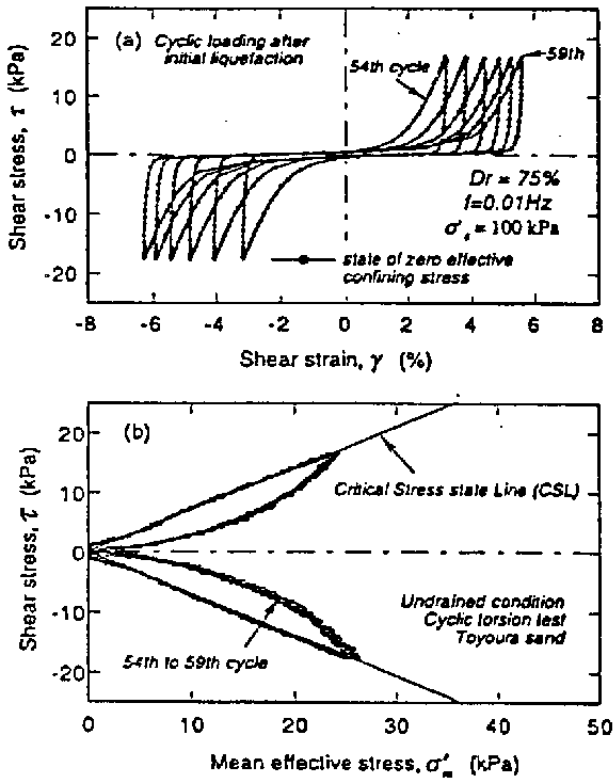

Figure 11. Post liquefaction shear stress-strain response (Shamoto et al. 1997).

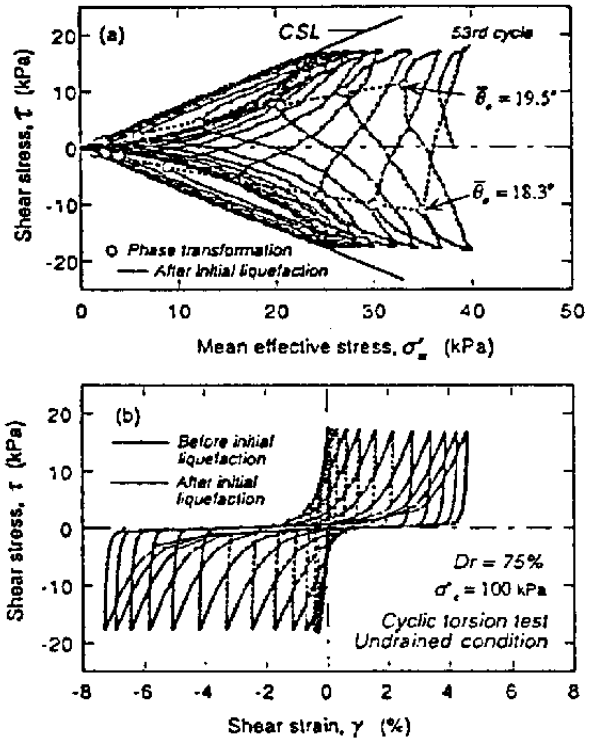

Figure 12a. Effective stress-path and stress-strain hysteresis observed in a cyclic undrained torsion test on saturated sand (Zhang et al. 1997).

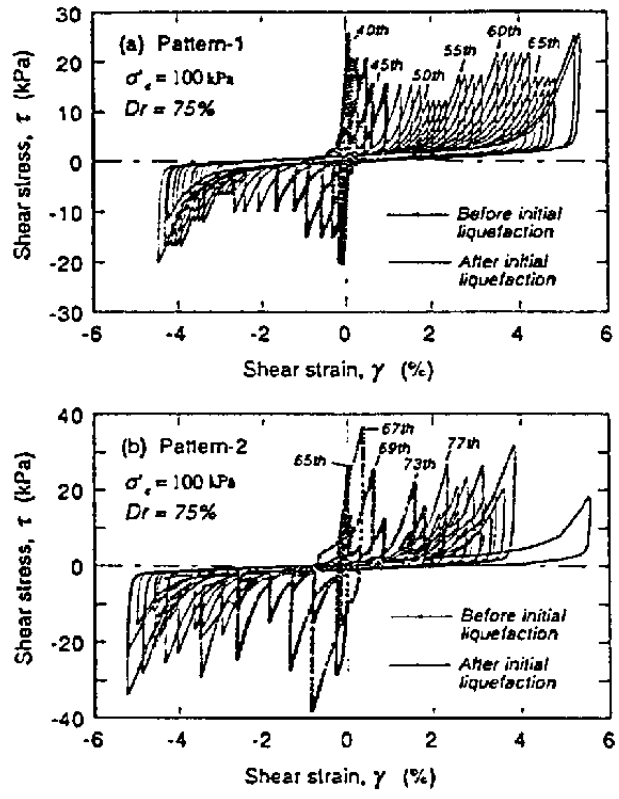

Figure 12b. Shear stress-strain relationship observed in undrained torsion tests for two patterns of irregular cyclic loading (Zhang et al. 1997).

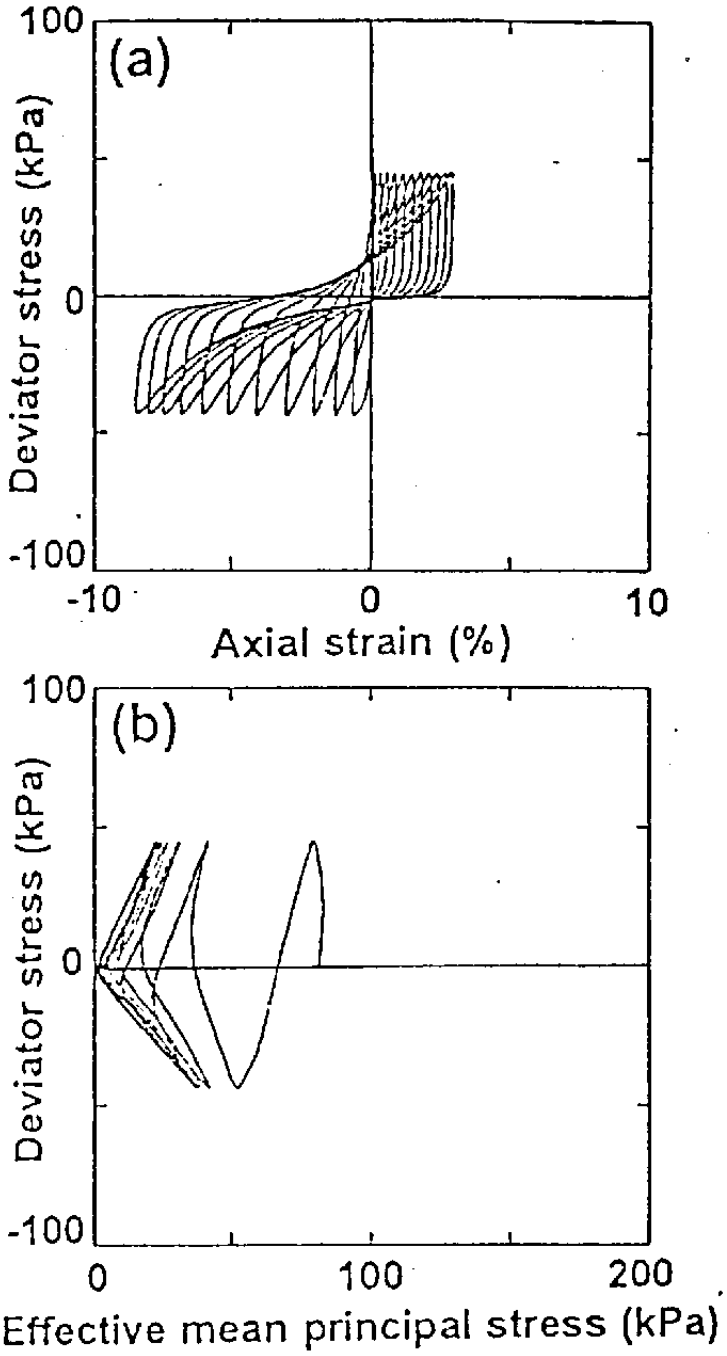

Figure 13. Stress-strain relationship and stress path for undrained cyclic triaxial test on gravely fill soil (Hatanaka et al. 1997).

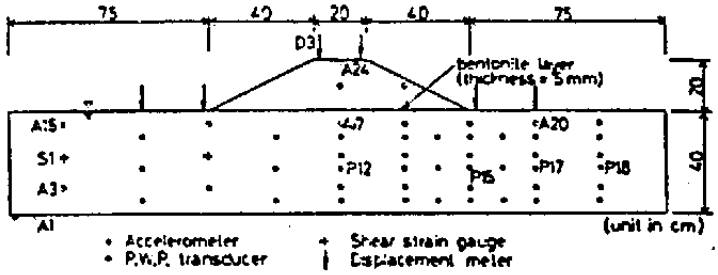

Figure 14a. Model configuration and transducer location (Koga and Matsuo 1990).

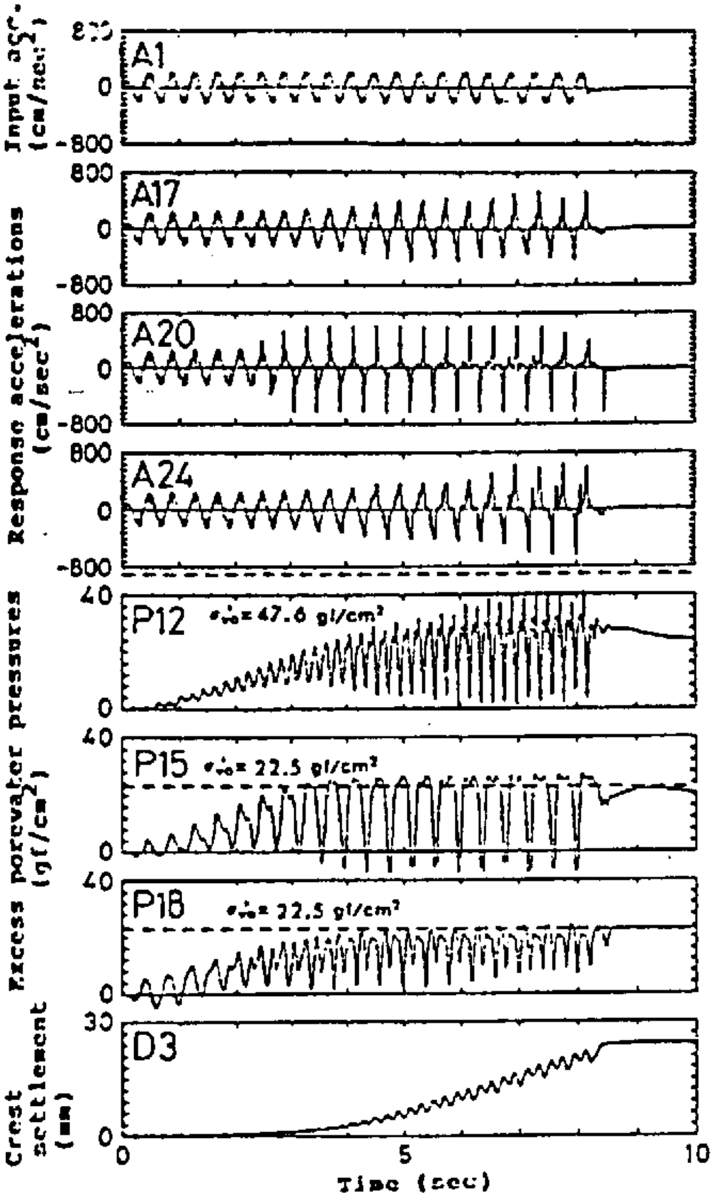

Figure 14b. Recorded time histories for base excitation of 220 gal (Koga and Matsuo 1990).

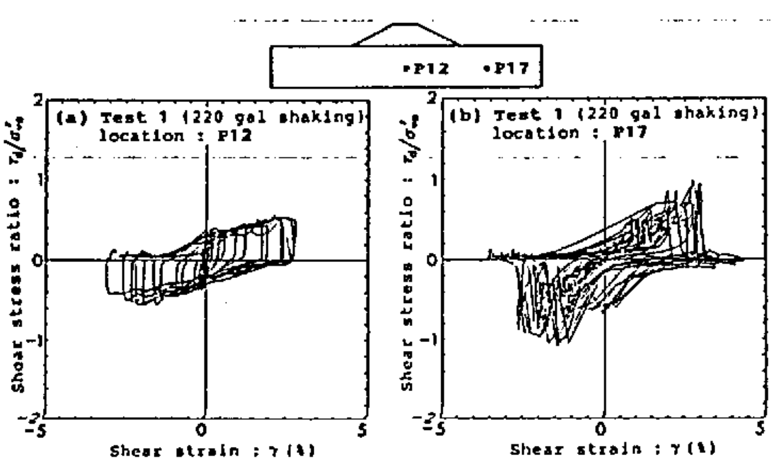

Figure 15. Calculated shear stress-strain histories (Koga and Matsuo 1990).

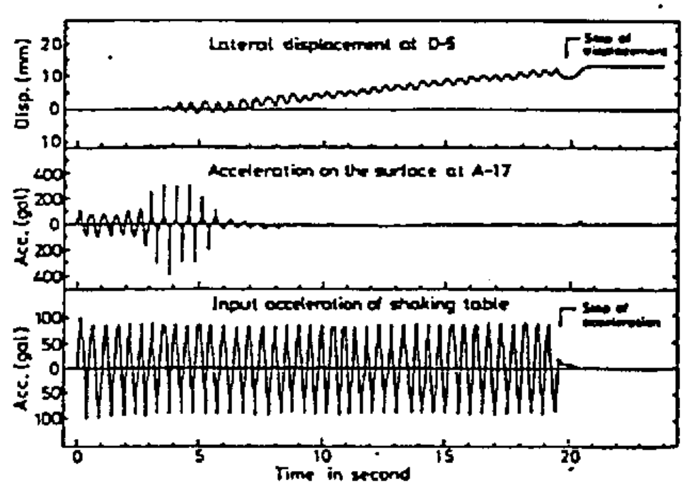

Figure 16. Time histories of acceleration and lateral deformations (Ishihara et al. 1991).

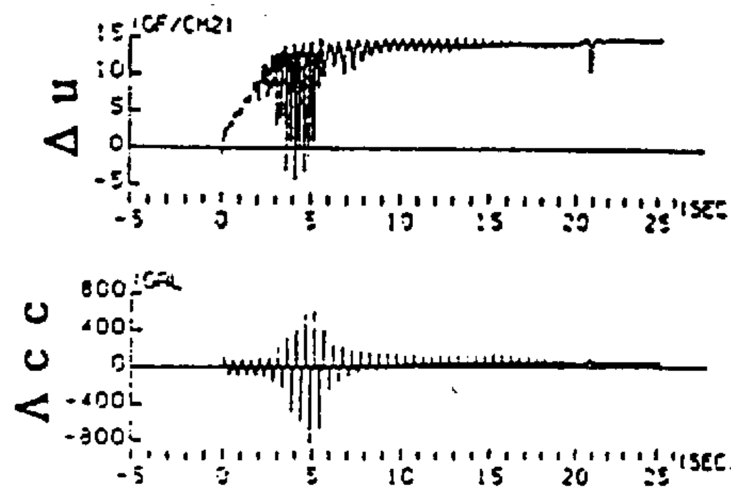

Figure 17. Time history of Behavior of ground (Sasaki et al. 1991).

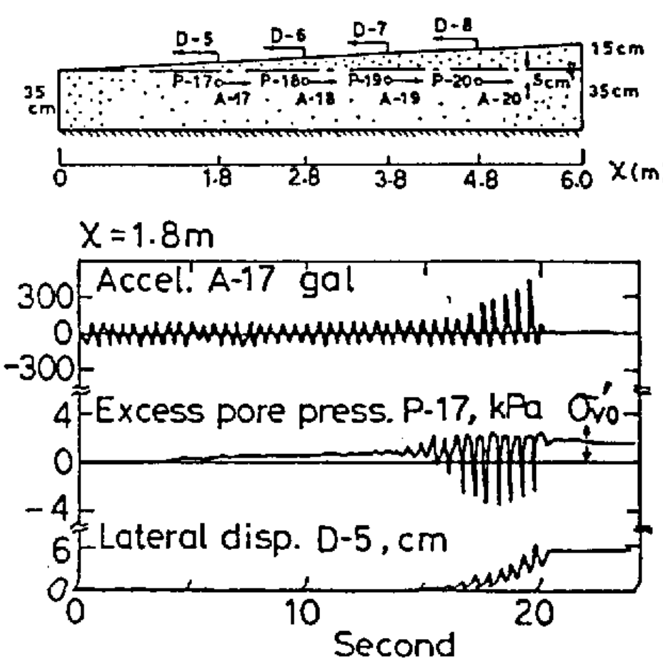

Figure 18. Time histories of recorded response (Sasaki et al. 1992).

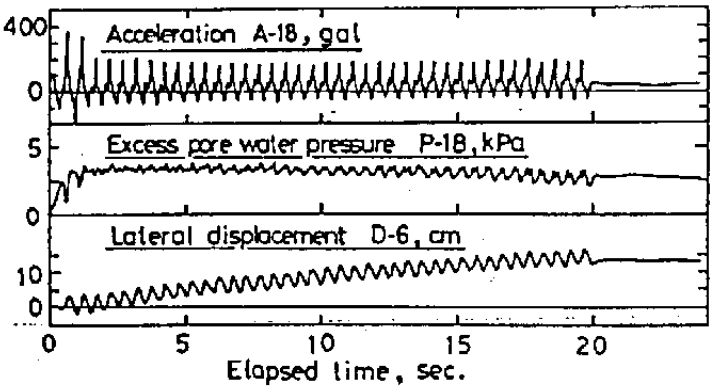

Figure 19a. Time histories of recorded response (Sasaki et al. 1992).

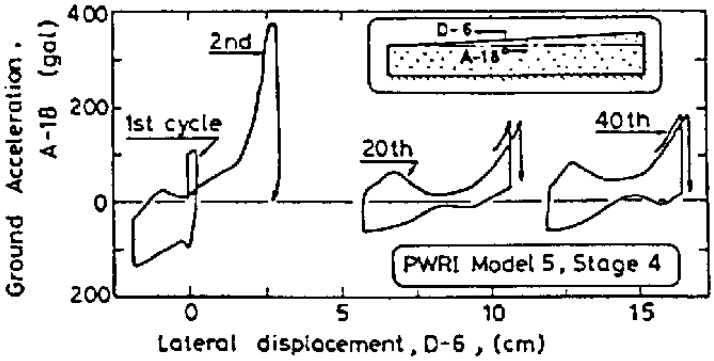

Figure 19b. Approximate idea of stress-strain relationship in liquefied layer (PWRI model 5, stage 4) (Sasaki et al. 1992).

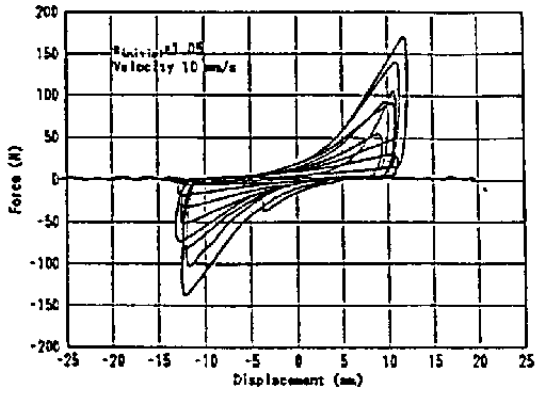

Figure 19c. Response of model pipe in liquefied ground (Towhata and Toyota 1994).

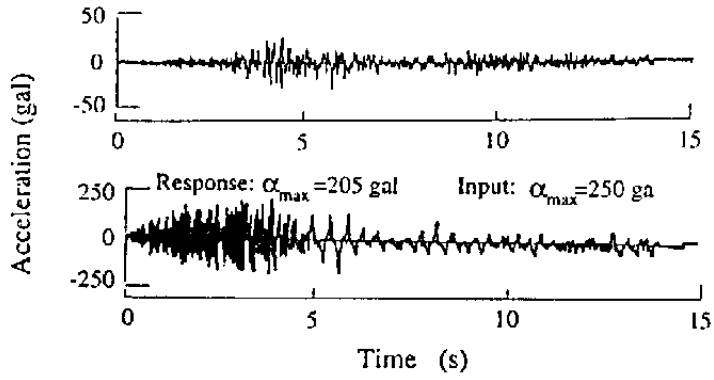

Figure 20. Time histories of input and ground surface response (Shamoto et al. 1996).

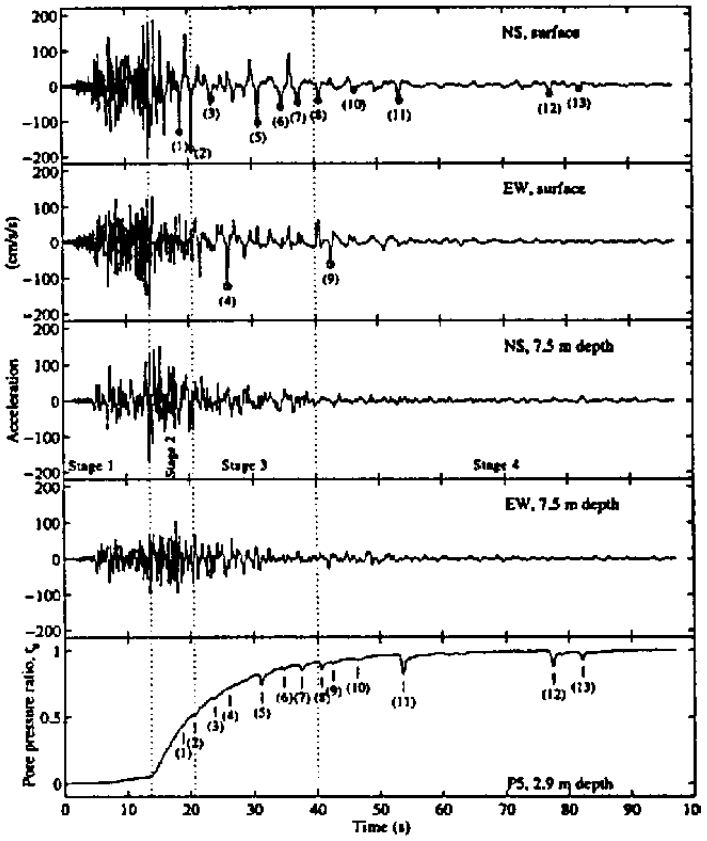

Figure 21. Recorded response at the Wildlife refuge site, Superstition Hills earthquake (Holzer et al. 1989).

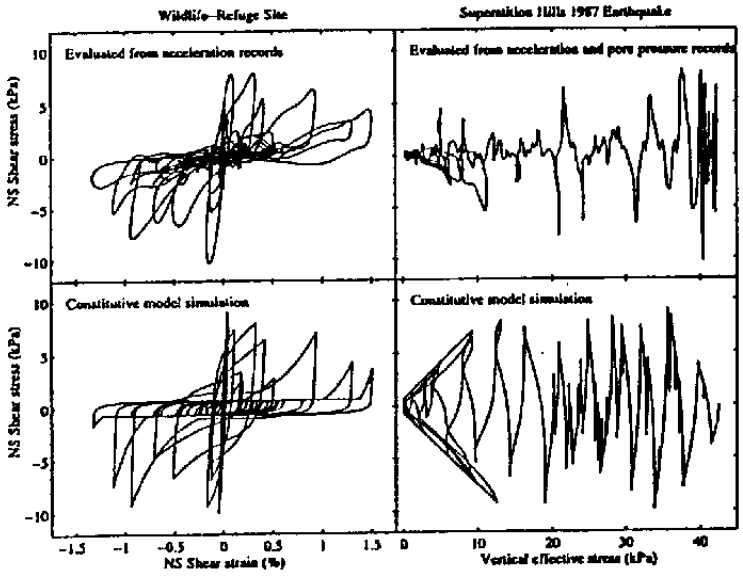

Figure 22a. Wildlife-refuge NS shear stress-strain and effective-stress histories during the Superstition Hills 1987 earthquake (evaluated from acceleration histories and computed by new constitutive model).

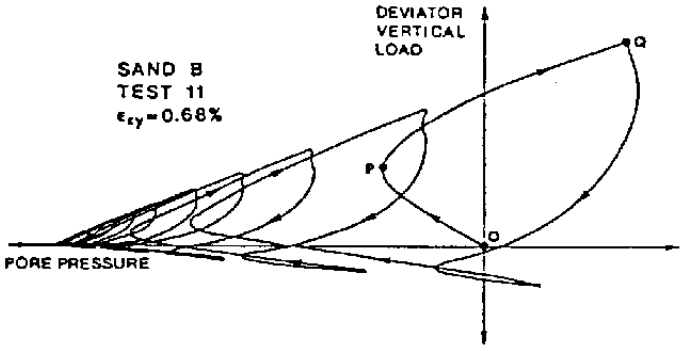

Figure 22b. Record of deviator vertical load versus pore pressure for test 11 (Vucetic and Dobry, 1988).

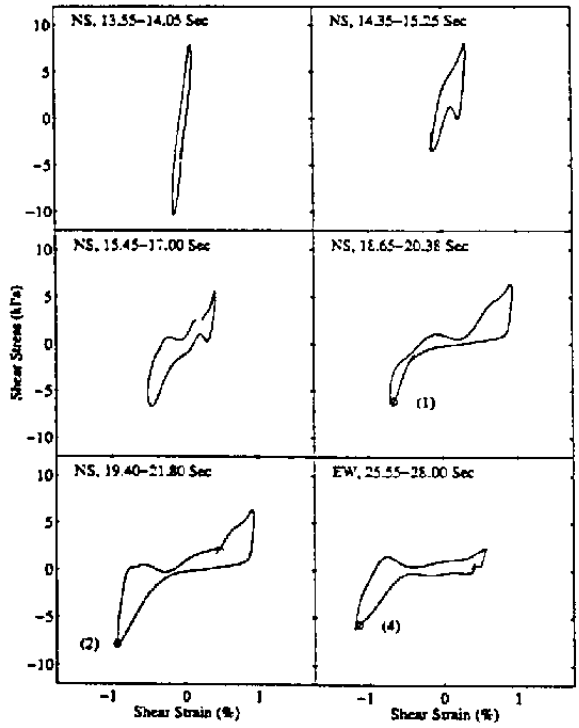

Figure 23. Selected Stress-strain loops of Wildlife-refuge response during Superstition Hills earthquake.

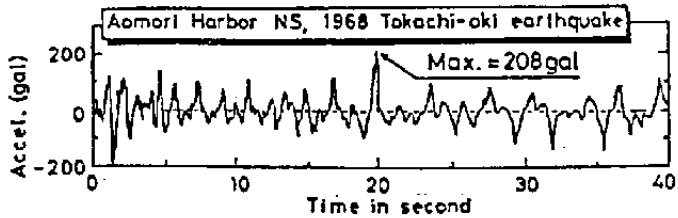

Figure 24. Aomori Harbor NS, 1968 Tokachi-oki earthquake (Towhata et al. 1996).

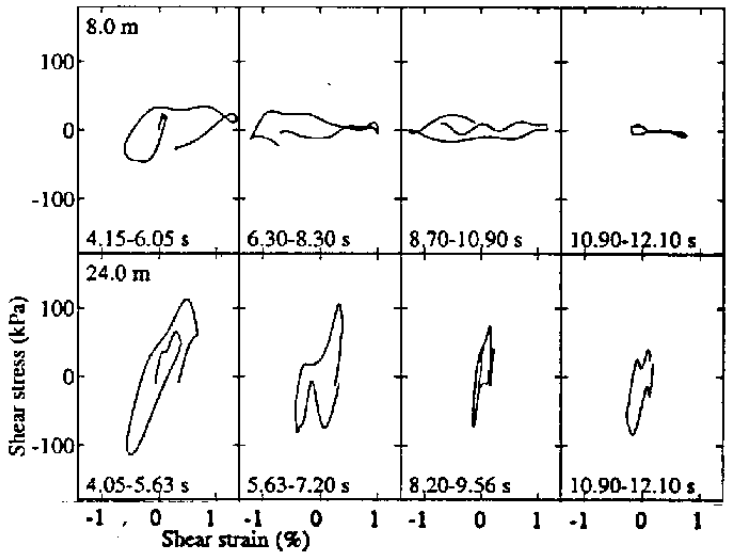

Figure 25. Selected stress-strain loops, Port Island, Hyogo-ken Nambu earthquake (Elgamal et al. 1995).

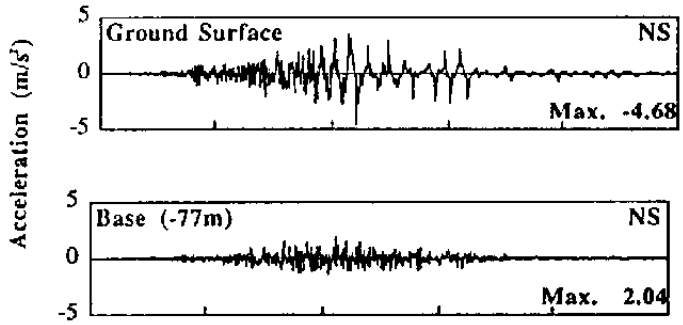

Figure 26. Recorded acceleration, Kushiro-oki earthquake 1993 (Iai et al. 1995).

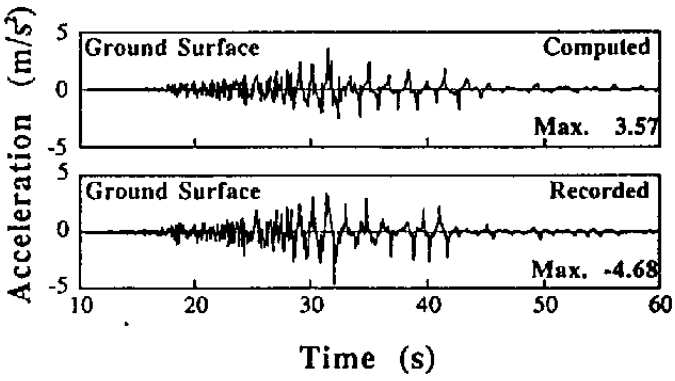

Figure 27. Recorded and computed accelerations at the ground surface (Iai et al. 1995).

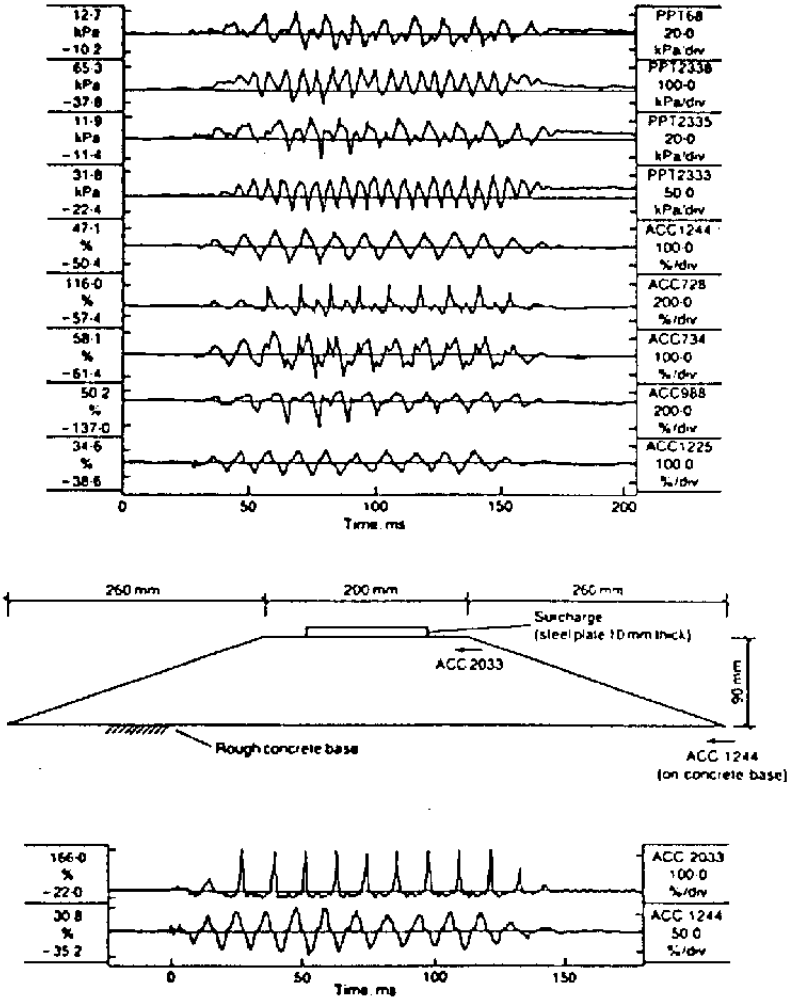

Figure 28. Recorded response in centrifuge test (Lee and Schofield 1988).

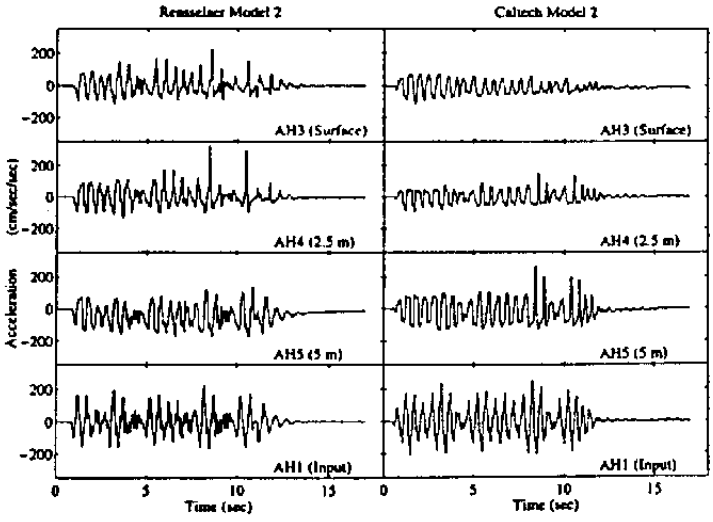

Figure 29. RPI and CalTech Model 2 acceleration histories at free surface (AH3(, 2.5m depth (AH4), and 5m depth (AH5), and input acceleration (AH1) at 10m depth (Taboada and Dobry 1993, Scott et al. 1993).

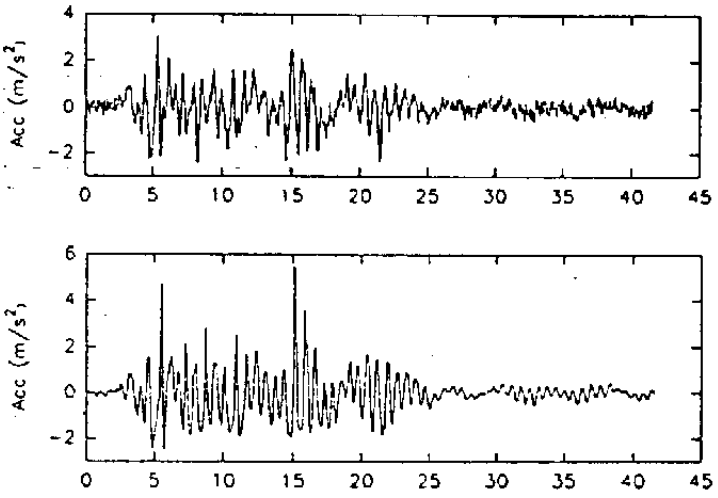

Figure 30. Recorded horizontal acceleration in UCD Model 7 (Wilson et al. 1993).

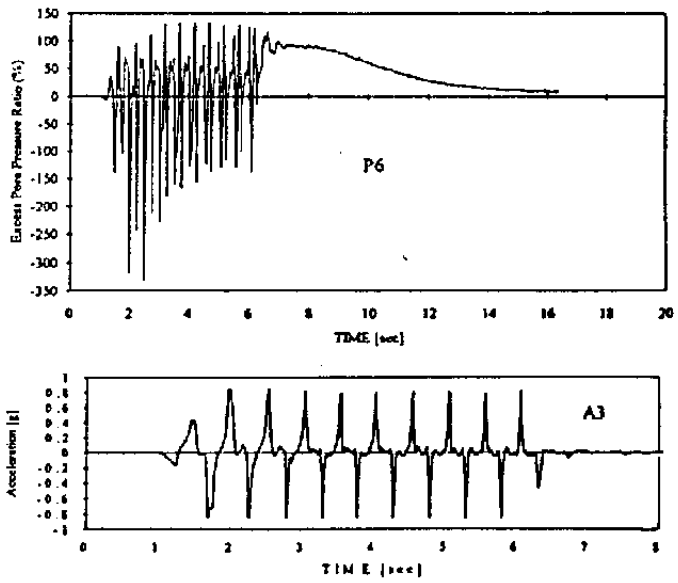

Figure 31. Pore-pressure and acceleration near surface of backfill, test 2e (Whitman and Ting 1994).

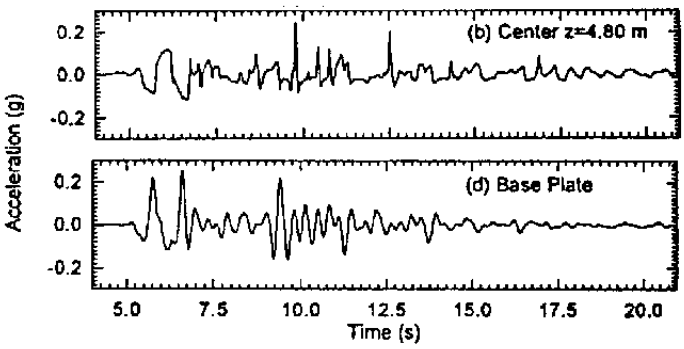

Figure 32a. Recorded lateral accelerations at UCD (Divis et al.1996).

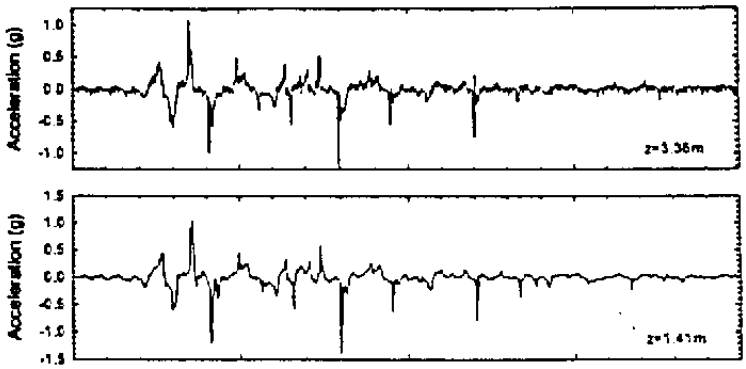

Figure 32b. Recorded acceleration response at UCD (Wilson et al. 1997).

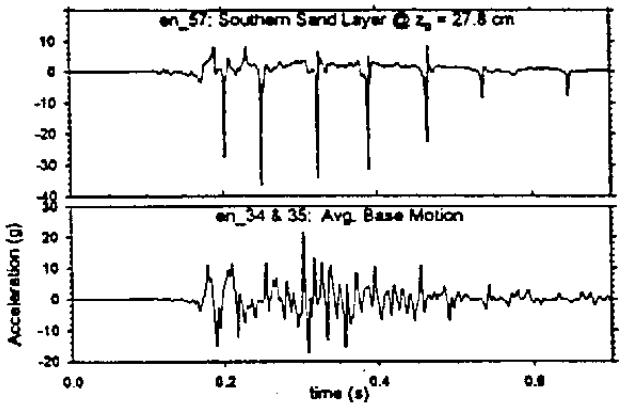

Figure 32c. Recorded acceleration response at UCD (Balakrishnan et al. 1997).

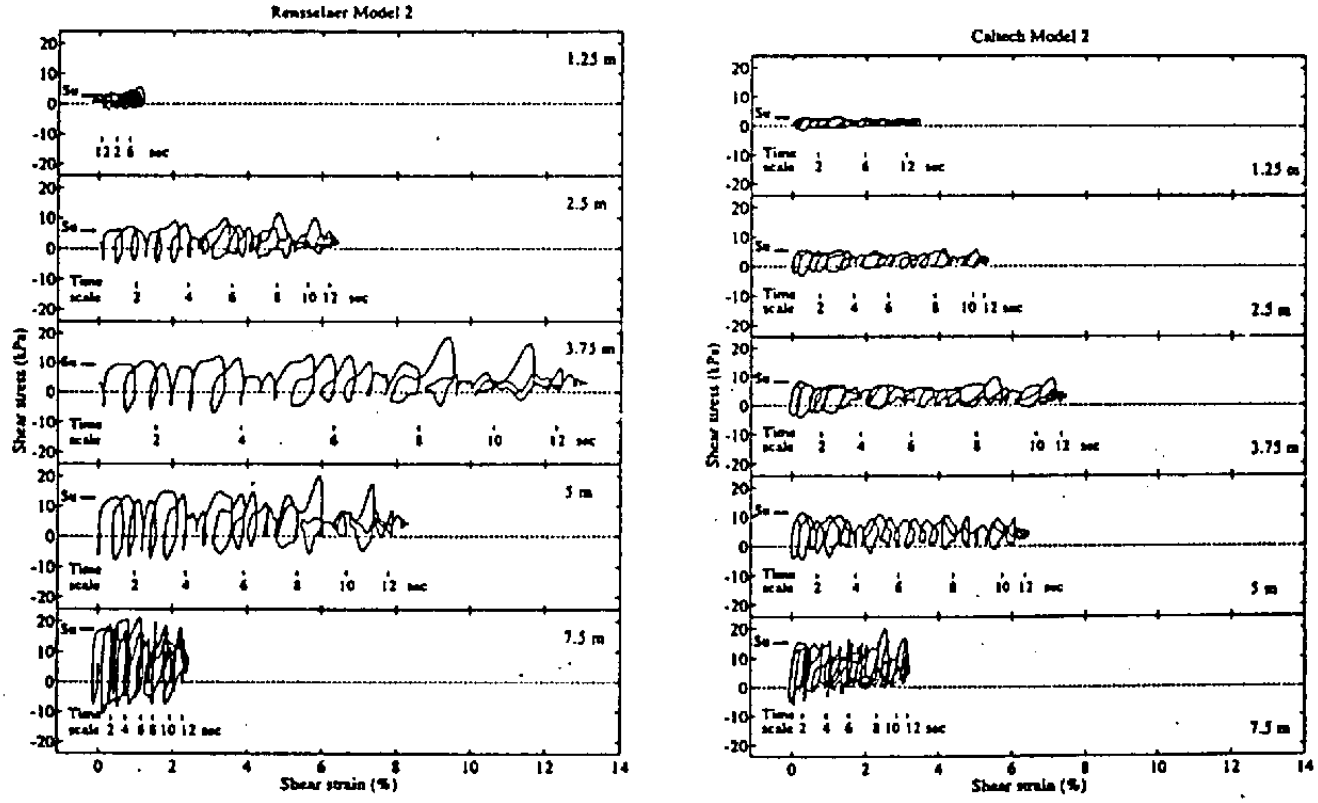

Figure 33. RPI and CalTech Model 2 shear stress-strain histories (Elgamal et al. 1996).

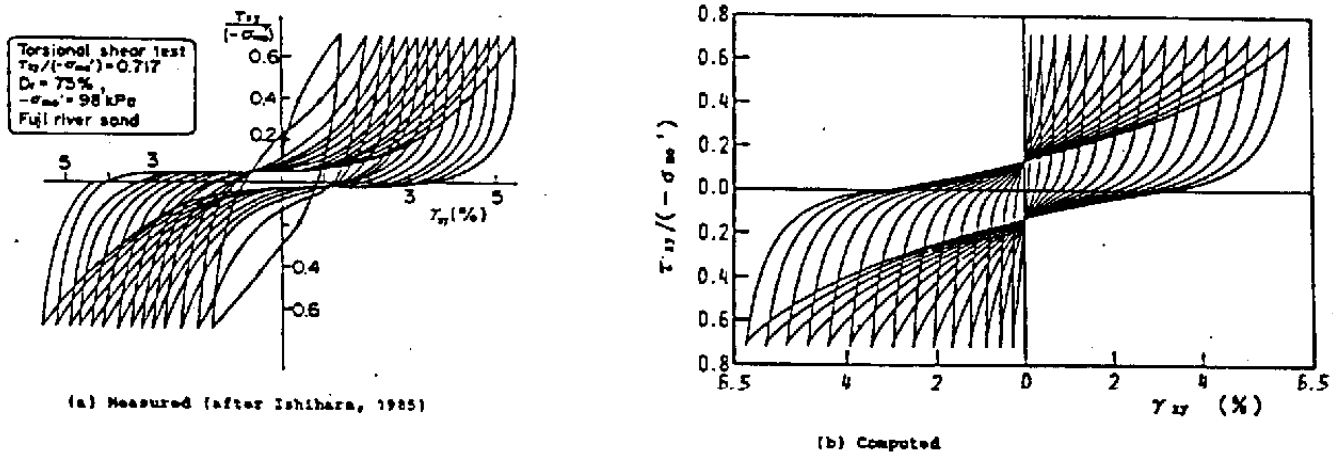

Figure 34a. Iai model performance and measured data (Iai 1991, Ishihara 1985).

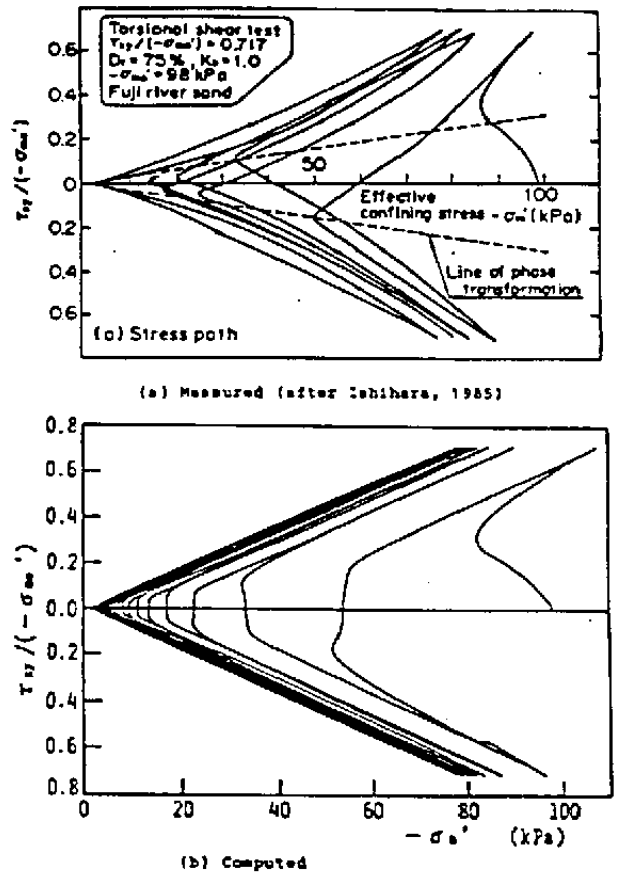

Figure 34b. Iai model performance and measured data (Iai 1991, Ishihara 1985).

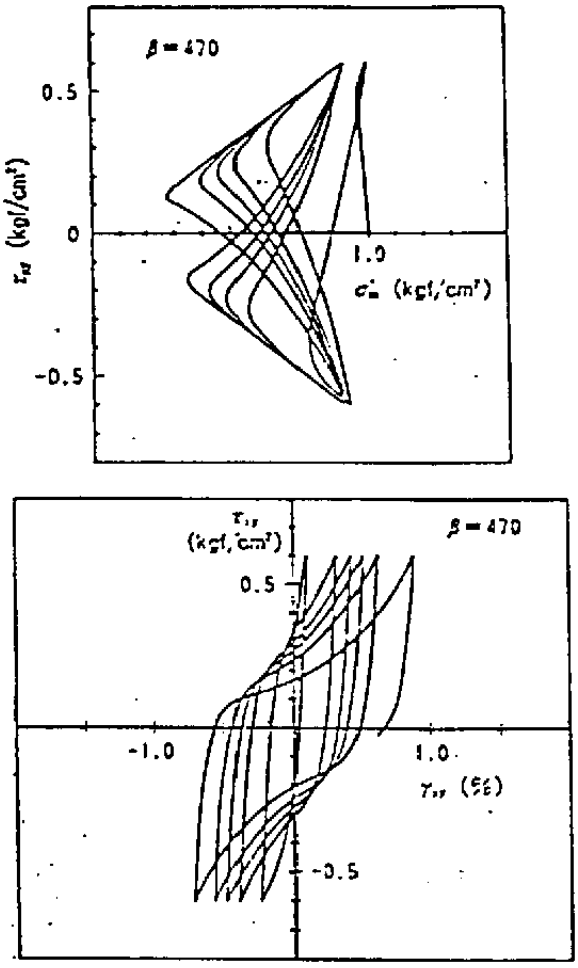

Figure 35. Computed results: effective stress path and shear stress-strain (Nishi and Kanatani 1990).

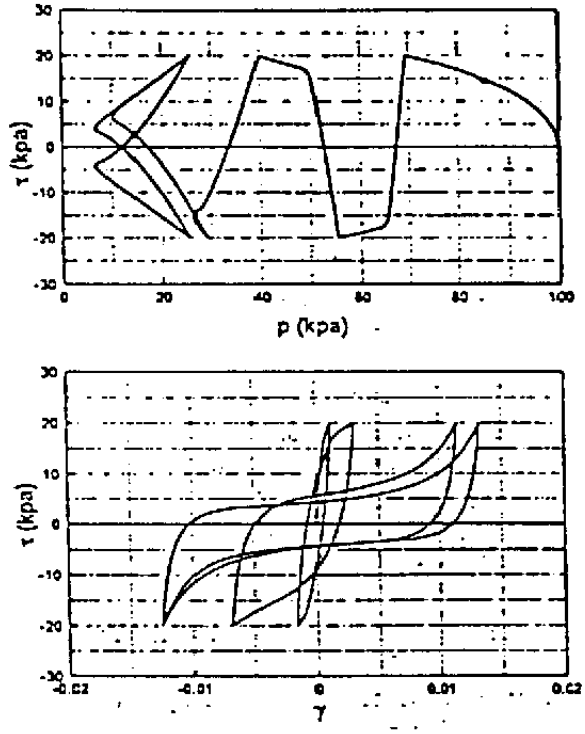

Figure 36. Undrained simple shear response (Li 1993).

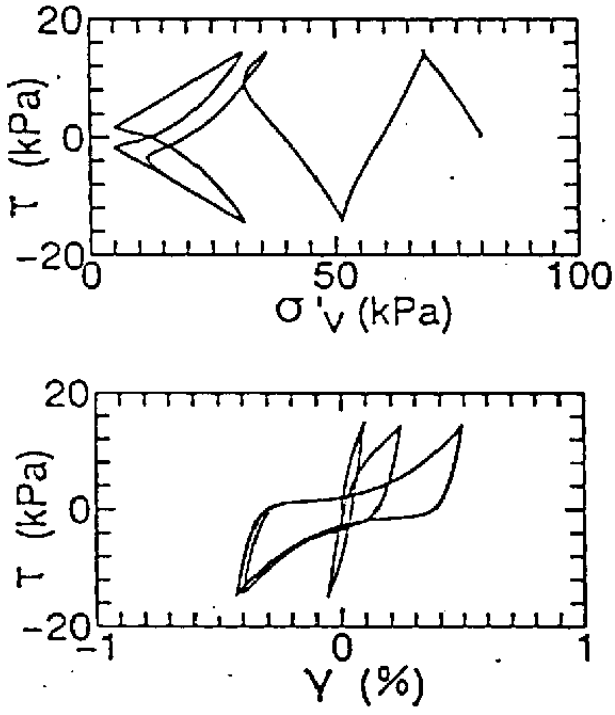

Figure 37. Effective stress path and shear stress-strain response (Kimura et al. 1993).

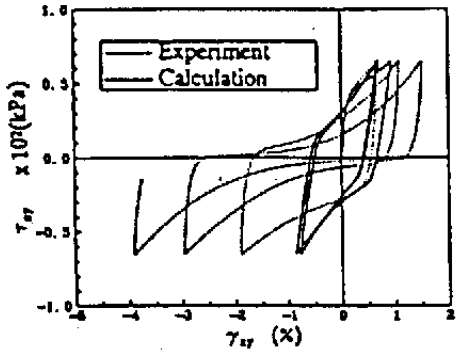

Figure 38. Simulation of shear stress-strain response (Tobita and Yoshida 1995).

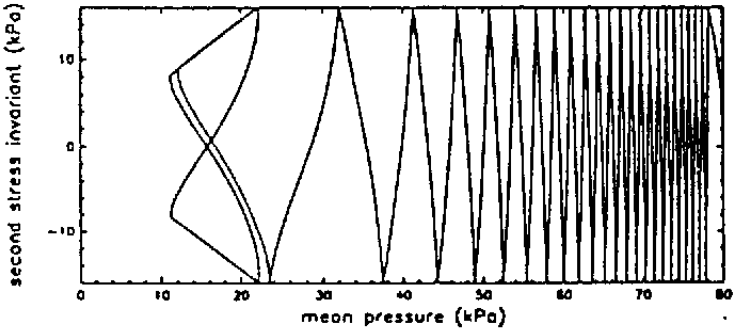

Figure 39. Predicted effective stress path (Bardet et al. 1993).

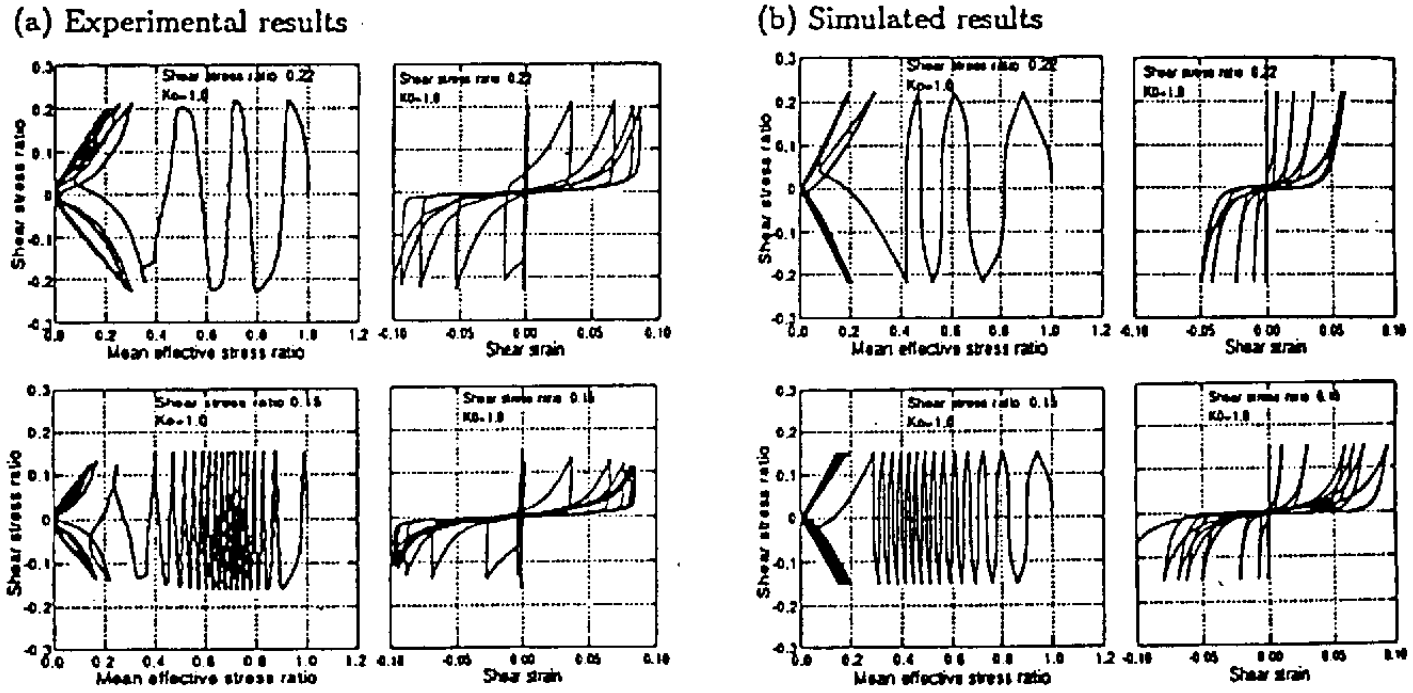

Figure 40a. Comparison between experimental and computer simulated response, Series A (Tateishi et al. 1995).

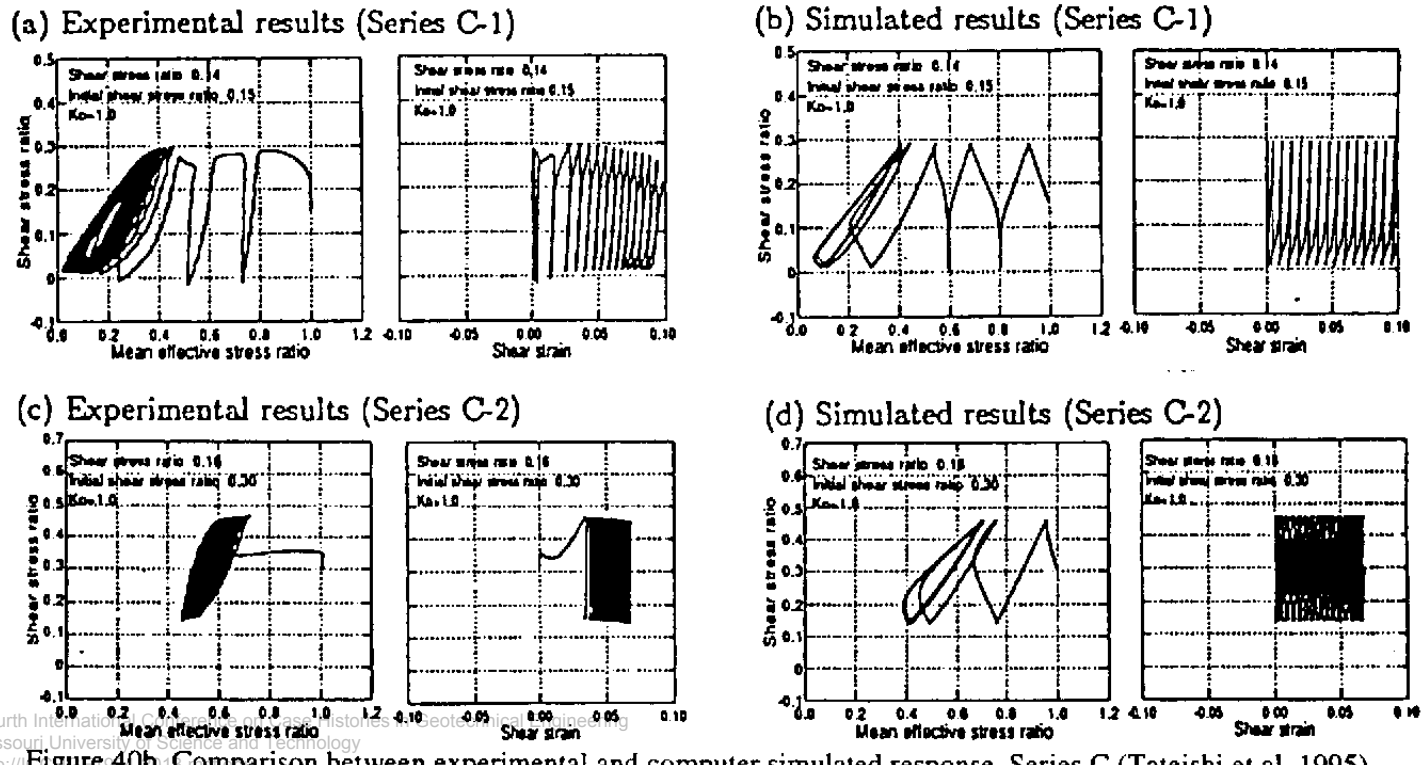

Figure 40b. Comparison between experimental and computer simulated response, Series C (Tateishi et al. 1995).

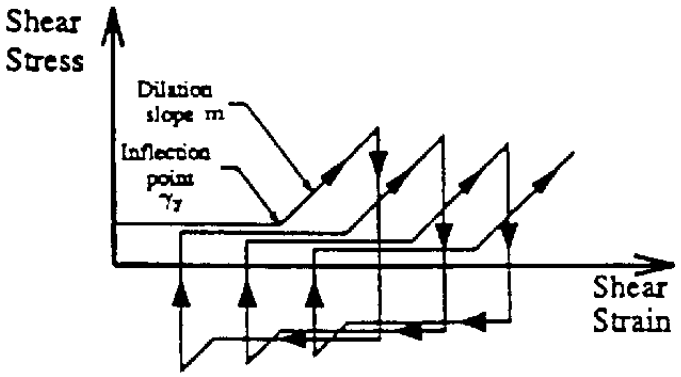

Figure 41. Simplified shear stress-strain relation (Abdoun 1994).

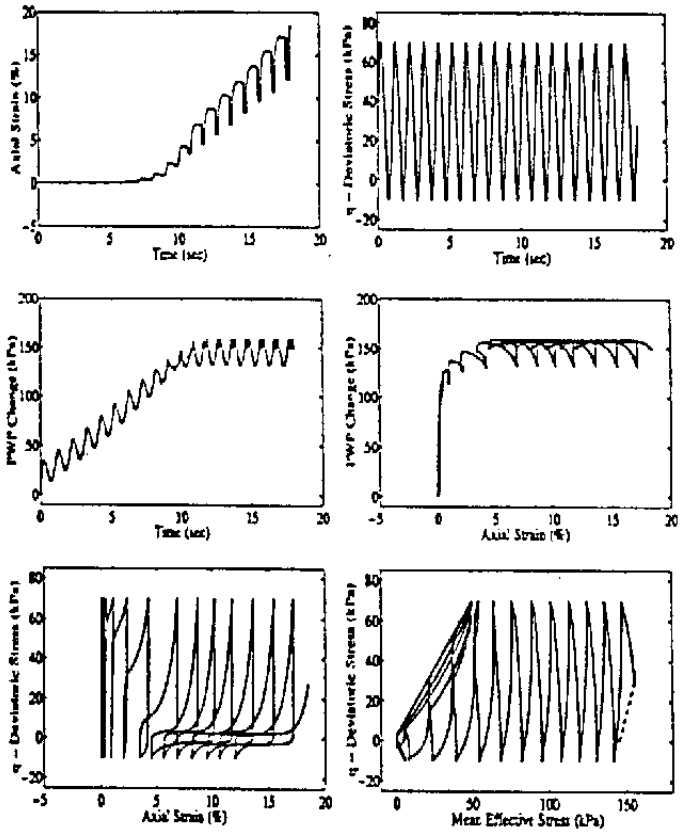

Figure 42. Simulation of cyclic triaxial undrained test with stress bias (Parra 1996).

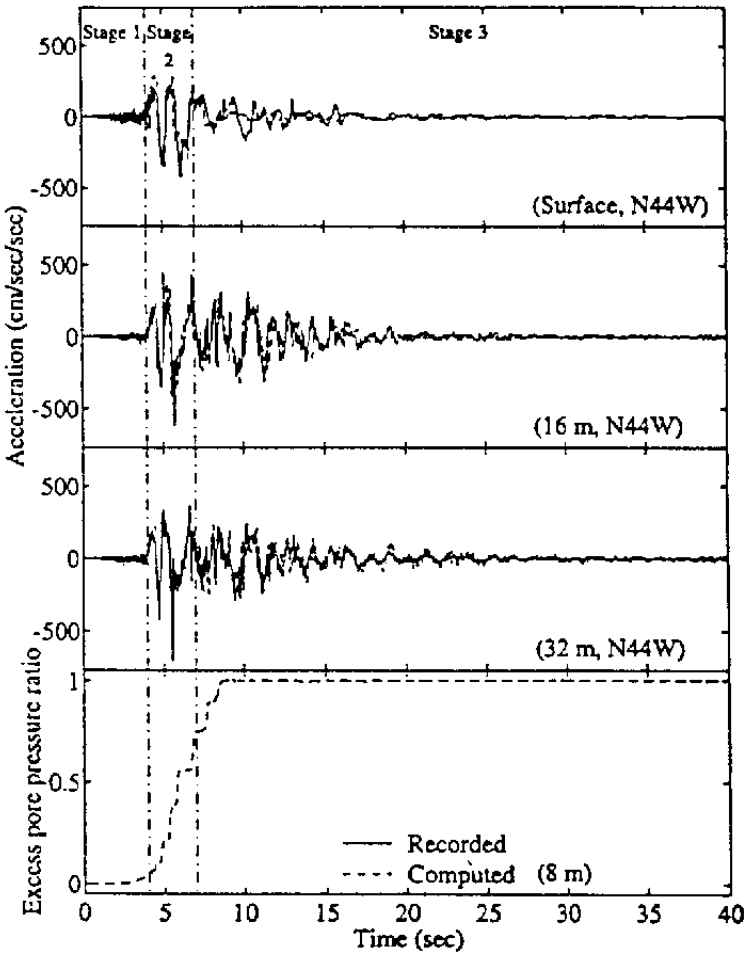

Figure 43. Port Island recorded and computed accelerations (Elgamal et al. 1996a).